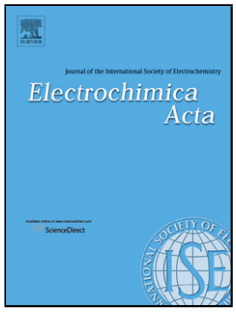

Title: Effect of combustion gas components on electrochemically promoted CO_2 capture performance of Pt/K-βAl_2O_3 at bench scale

Author: Esperanza Ruiz Pedro J. Martínez Ángel Morales Gema San Vicente Gonzalo de Diego José M. Sánchez

PII: S0013-4686(15)30920-8
DOI: http://dx.doi.org/doi:10.1016/j.electacta.2015.11.145
Reference: EA 26145

To appear in: *Electrochimica Acta*

Received date: 14-5-2015
Revised date: 21-10-2015
Accepted date: 30-11-2015

Please cite this article as: Esperanza Ruiz, Pedro J.Martínez, Ángel Morales, Gema San Vicente, Gonzalo de Diego, José M.Sánchez, Effect of combustion gas components on electrochemically promoted CO2 capture performance of Pt/K-*rmbeta*Al2O3 at bench scale, Electrochimica Acta http://dx.doi.org/10.1016/j.electacta.2015.11.145

Effect of combustion gas components on electrochemically promoted CO_2 capture performance of Pt/K-βAl_2O_3 at bench scale

Esperanza Ruiz* esperanza.ruiz@ciemat.es, Pedro J. Martínez, Ángel Morales, Gema San Vicente, Gonzalo de Diego, José M. Sánchez

Centro de Investigaciones Energéticas, Medioambientales y Tecnológicas (CIEMAT), Av. Complutense, 40, 28040 Madrid, Spain

*Corresponding author: Tel.:+34-91-346-0887; fax.:+34-91-346-6269.

Abstract

Due to the continuous increase in CO_2 atmospheric levels resulting from fossil fuels combustion, it is necessary to develop new, more efficient and less-energy intensive processes, that allow economically and selectively separate CO_2 without the negative impact of co-existing gases (H_2O, SO_2, NO, etc.).

This work presents a bench-scale study of the effect of combustion gas components on the electropromoted CO_2 capture performance of an easily scalable Pt/K-βAl_2O_3 tubular electrochemical system, at high flow rates and in the presence of representative amounts of O_2, H_2O, SO_2, NO and N_2O.

On the basis of previous mechanistic and spectroscopic studies, cyclic voltammetry studies showed that the system is able to capture CO_2, not only by electropromoted adsorption but also as carbonates/bicarbonates by potassium ions electrochemically supplied to Pt surface. CO_2 capture is enhanced in the presence of O_2 and H_2O. The CO_2 capture behaviour of the system is almost unaffected by the presence of N_2O. SO_2 poisons CO_2 capture, whereas the presence of NO appears to considerably hinder CO_2 capture. The Pt/K-βAl_2O_3 system can be regenerated, allowing CO_2 separation, by electrochemical decomposition of previously stored compounds without increasing temperature, with the consequent energy saving.

Keywords: Electrochemical promotion; bench scale; CO_2 capture; Pt/K-βAl_2O_3; combustion exhaust.

Introduction

Control of carbon dioxide emissions from fossil fuel combustion power plants may become necessary to minimize global warning produced by the greenhouse effect. Physical adsorption of CO_2 is a promising approach for CO_2 capture from combustion flue gases. The main challenge for this technology is currently the development of new, more efficient and less-energy intensive systems, that allow economically and selectively separate CO_2 without the negative impact of co-existing gases (H_2O, SO_2, NO, etc.) [1]. As a result, it has been proposed the development of regenerable solid adsorbents (alumina, activated carbon, etc.) chemically promoted with various agents (alkali or alkaline-earth cations, etc.) during their preparation procedure [1]. The use of electrochemical promotion of catalysis (EPOC) constitutes, in principle, a novel alternative to improve CO_2 capture by "in-situ" addition of the chemical promoter during the adsorption process, due to electrochemical pumping of ions from the solid electrolyte to the surface of the working-catalyst electrode, which act both as CO_2 chemisorption promoters and storing components [2, 3]. In addition, not only CO_2 capture but also regeneration can be monitored and controlled by electrochemical means, allowing optimising the duration of both sequences [3] and system regeneration without increasing temperature, with the consequent energy saving.

The prominent methods of carbon dioxide capture by adsorption, using pressure and temperature swing processes, have thermodynamic limitations that result in low efficiencies and unacceptable added energy costs. New technologies, which are not reliant on pressure and temperature swing processes, are needed to reduce the costs associated with the direct capture of CO_2. The electrochemical swing adsorption process proposed appears to be a promising approach for the post-combustion capture of CO_2 since it does not require significant heating and subsequent cooling of the adsorbent for regeneration and preparation for the next sorption

cycle. Moreover, even though CO_2 capture by electrochemical swing adsorption does require the application of an electric current, the amount of current is less than that required to compress the gas for conventional pressure swing adsorption, resulting in net efficiency gains. Therefore, electrochemically promoted adsorption offers an isothermal and less energy intensive alternative to the thermal and pressure swing adsorption strategies typically used for CO_2 capture. Moreover, due to the ease of integration and installation reported for electrochemically driven separation processes [4], the technology could be potentially applied for sequestering CO_2 in fossil fuel fired power plants, resulting in significant decrease in total energy consumption associated with CO_2 capture and in potential energy cost savings.

The driving force in these systems is supplied by changes in electrochemical potential, inducing changes in potassium promoter surface coverage and then in the relative binding strength of chemisorbed CO_2 [2], which enables to modulate and control CO_2 capture and release by CO_2 adsorption and potassium carbonate/bicarbonate formation and decomposition, respectively. These potential changes can be controlled precisely to reduce energy losses. Moreover, both electropromoted CO_2 capture and regeneration process can be online monitored by a simple measurement of the electrical current generated by the applied polarization, without the need to analyse CO_2 gas content [3].

From the best of our knowledge, the studies to date [3, 5–6] have focused on the study of electropromoted CO_2 adsorption under simplified exhaust gas compositions. However, from an industrial perspective, especially for CO_2 derived from coal-fired power plant effluents, it is inevitable that other gaseous pollutants, such as SO_2, NOx, N_2O, etc., will be present in addition to CO_2. Moreover, there are some scale-up facets, such as operation at high flow rates, under realistic gas compositions and using catalyst-electrode configurations easily adaptable to the existing devices (conventional flow reactors), that need to be tackled in more depth for the potential practical application of this technology [7].

This work presents a bench-scale study of an electrochemically activated CO_2 capture process under conditions representative of combustion exhausts, i.e., at high flow rates and in the presence of representative amounts of O_2, H_2O, SO_2, NO and N_2O, over an easily scalable Pt/K-βAl_2O_3 tubular electrochemical system.

Cyclic voltammetry can be used for the investigation of phenomena involved in adsorption and reaction processes on Pt electrodes [8–11]. The use of cyclic voltammetry to study electrochemical processes taking place in the Pt/Na- βAl_2O_3 system under different gas environments has been recently reviewed [6]. In the present work, this technique has been applied for the study of CO_2 adsorption and formation of potassium compounds upon electrochemical pumping of potassium ions to the Pt surface of Pt/K-βAl_2O_3 in the presence of representative amounts of O_2, H_2O, N_2O, SO_2 and NO using the best operating conditions identified in a previous work [12].

1. Experimental

1.1 Electrochemical catalyst

The Pt/K-βAl_2O_3/Au single chamber electrochemical cell tested in the present work consisted of a thin Pt film (catalyst-working electrode) deposited on the outer surface of a 28-mm-i.d., 100-mm-long, and 1-2 mm-thick K-βAl_2O_3 tube, closed flat at one end (IONOTEC).

A gold counter electrode was deposited on the inner side of the solid electrolyte tube to allow polarizations, given that gold is reported [13] to be inert in the process. It was prepared by painting the inner side of the K-βAl_2O_3 tube with a gold paste (HERAEUS-C5729). The deposited paste was dried at 150 ºC during 10 min, heated to 850 ºC at a controlled rate and, finally, annealed at 850 º C during 10 min.

The Pt film was prepared, as described previously [12, 14], by two consecutive dip-coating steps with intermediate calcination at 850 ºC. The K-βAl_2O_3 tube was dipped into a Pt precursor solution, drawn up at a constant speed, dried and fired at about 600 ºC during 1 hour. Pt precursor solution was prepared according to a CIEMAT European patent [15].

The final Pt loading was 0.86 mg Pt/cm^2 [12]. Pt dispersion was estimated from the average Pt crystal size evaluated from X-ray broadening of the main Pt diffraction peak and the Debey-Scherrer equation [14] and resulted to be 2.4 %. The surface mol (mol of active sites) of the Pt film was calculated using the estimated dispersion and the known Pt loading values and resulted to be 1.05 x 10^{-5} mol Pt.

1.2 Catalyst characterisation

A small fragment of the electrochemical catalyst was characterized, both as prepared and after testing, by X-Ray Diffraction (XRD) and X-ray Photoelectron Spectroscopy (XPS) techniques.

XRD patterns of the catalyst-working electrode film were recorded on a PHILIPS "Xpert-MPD" instrument using a Cu Kα X-ray source (45 kV and 40 mA), a 2θ range of 15-75º, a step size of 2θ=0.03º and a step time of 2 s.

The surface chemical composition of the catalyst electrode film was examined by XPS using a Perkin-Elmer PHI 5400 System equipped with a Mg Kα (hν = 1253.6 eV) excitation source running at 15 kV and 20 mA and having a beam diameter of 1 mm. Base pressure in the analysis chamber was maintained at about 10^{-9} Torr. The pass energy was set at 89.5 eV for general spectra (0-1100 eV) and at 35.75 eV for high resolution spectra. The energy scale was referenced to the carbon 1s signal at 285.0 eV.

1.3 Bench-scale plant

Electropromoted CO_2 adsorption/desorption cycles were carried out in a bench-scale plant described in detail elsewhere [14]. It is able to treat up to 20 m^3 h^{-1} (at 273 K and 1 atm) of gas with temperatures ranging between 250 and 450 ºC, at about atmospheric pressure. Combustion exhaust gas components are supplied, as synthetic gases (AIR LIQUIDE), by electronic mass flow controllers (Bronkhorst HIGH-TECH). Steam can be added to the gas mix by vaporising water fed into a boiler by a metering pump (Dosapro Milton Roy). Other potential liquid gas components (HCl, etc.) can be also fed by a metering pump (ProMinent Gugal, S.A.). The mixed wet gas is then preheated in an oven (KHANTAL) and sent to a fixed-bed down-flow quartz reactor, with 35 mm of diameter and 900 mm of length, heated by a three-zone electrical furnace (CARBOLITE). The adsorption temperature was determined with an alumina sheathed chromel-alumel thermocouple placed close to the electrochemical catalyst. An electronic differential pressure transmitter measures the pressure drop across the reactor. Polarizations across the tubular electrolyte cell were imposed and measured by a potentiostat-galvanostat Voltalab 21 (Radiometer Analytical).

1.4 Gas analysis system

As reported previously [12, 14], the composition of the gas mixtures entering and leaving the reactor was determined using a gas micro-chromatograph (VARIAN CP-4900) in conjunction with a NDIR CO_2/CO (FUJI ELECTRIC ZKJ) and a chemiluminescence (TOPAZE-32S ENVIRONMENT) on line analysers.

As described previously [12, 14], the gas micro-chromatograph (VARIAN CP-4900) is equipped with three column modules: a PLOT Molecular Sieve 5Å (10 m x 0.32 mm), a

PORAPLOT Q (10 m x 0.15 mm) and a CP-SIL 5 CB (6 m x 0.15 mm), using helium as carrier and reference gas for the thermal conductivity detectors. These enabled the analysis of N_2, CO_2, O_2 and other exhaust gas constituents as NO, N_2O, NO_2, CO and SO_2.

1.5 Operating conditions and procedure

The electrochemical catalysts were placed inside the quartz reactor with the closed flat end of the tube facing the inlet gas stream, in order to improve catalyst-gas contact and to minimize by-pass phenomena. The electrical connections in the reactor were made from gold wires (HERAEUS), since gold is reported to be catalytically inert in the process [13].

Before the electropromoted CO_2 capture experiments, the catalyst was reduced in a stream of H_2 at 400 ºC during 1 h in order to ensure that the platinum is in its metallic form.

The concept of electrochemical promotion is based on the fact that a direct correspondence exists between the promoter coverage over catalyst surface and the value of the applied potential, i.e., the application of different polarizations allows controlling the amount of potassium ions electrochemically transferred to the Pt film, inducing changes in the binding strength of chemisorbed species and modifying the competitive adsorption of the different coexistent gases [2]. In accordance with previous studies [16–18], on working with cationic electrochemical catalyst, the application of a high positive catalyst potential allows maintaining the Pt surface free of electropositive ions (unpromoted conditions). Therefore, before each test the Pt catalyst-electrode surface was electrochemically cleaned by pumping potassium ions, which might thermally migrate to the Pt film, back to the solid electrolyte (unpromoted reference state) via holding the catalyst potential at 4 V during 30 min under the same reactive atmosphere. At the end of this time the current density fell to practically zero.

However, a decrease in the applied potential to negative values involves that potassium promoter ions are electrochemically transferred to the Pt catalyst electrode, giving rise to a progressive increment on promoter coverage, and, thus, to electropromotion of the catalyst surface (electrochemically promoted conditions). This addition of an electropositive promoter (K +) gives rise to a reduction in the catalyst work function, disadvantaging the chemisorption of electron donor (electropositive) species, while, at the same time, promoting the adsorption of electron acceptor (electronegative) species. There is a certain scale of electronegativity or electron acceptor capacity. Thus, depending on the electronegative or electropositive nature and magnitude of the different coexistent adsorbates, and on which is in excess on the surface of the catalyst, polarisation will have a positive or negative effect on the adsorption and reaction with promoter species of the different coexistent adsorbates over the catalyst-electrode surface.

The system was studied on consecutive electropromoted adsorption-desorption cycles (up to three) under different gas compositions.

Cyclic voltammetry is reported [6] to allow the investigation of the phases formed upon electrochemical pumping of promoter ions to the catalyst surface. In the present study, cyclic voltammetry has been used for the study of CO_2 adsorption and potassium carbonate/bicarbonate formation and decomposition during the electrochemically promoted CO_2 capture process on the Pt surface, by monitoring of the electrical current generated by the applied cyclic polarization, under different conditions. The appearance of peaks during the forward (application of decreasing potentials) or backward (application of increasing potentials) scan may be related to the migration of the promoter to (forward or cathodic scan) or from (backward or anodic scan) the surface of the Pt electrode and with the formation or decomposition of promoter species or any other chemical compound between the promoter

and the adsorbates present on the surface of the electrocatalyst. Therefore, the area of these negative and positive peaks is proportional to the amount of CO_2 (or other adsorbate) captured and released, during the cathodic and anodic scans, respectively.

The area of the cathodic and anodic peaks corresponds to the electric charge passed between the working and counter electrodes for the cathodic and anodic scan, respectively. The corresponding coverage of potassium species (θ_K) established on the Pt surface for each scan can be calculated according to Faraday's law (Eq. 1) [6, 19] by integration of the current density versus time, or equivalently, versus potential curves obtained for the cathodic and anodic scan, respectively.

$$\theta_K = \int \frac{I}{FN} dt = \frac{A}{FN} \int j dt \quad (1)$$

Where I is the current, F is the Faraday's constant, N is the surface mol (mol of active sites) of the Pt catalyst electrode, A is the superficial surface area of the electrode/electrolyte interface and j is the current density. It is possible to confirm the reversibility of the electropromoted process by comparison of θ_K calculated for each scan, because the obtainment of similar values of θ_K for both scans corroborates the fact that most of the amount of potassium electrochemically pumped to the Pt surface during the cathodic scan participates in the formation of phases which are decomposed during the anodic scan [6, 19]. Comparison of θ_K corresponding to each pair or combination of cathodic and anodic peaks, ascribed to the formation/decomposition of surface compounds, by performing the integration only for the currents in the potential range where the formation/decomposition of these surface compounds occurs, has been also attempted. However, in this case, there is a large uncertainty concerning the determination of the area (related with the baseline to be used in the calculation of each peak area) and, thus, of the corresponding potassium coverage for very small (or even indiscernible), very wide or not well formed peaks.

The results of the cyclic voltammetry studies can be rationalized considering the effect of varying applied potential on the chemisorptive bond strength of coexistent adsorbates [2] and in accordance with the mechanisms for CO_2 (or N_2O, NO, SO_2 and H_2O) adsorption and reaction and with the identity of the potassium phases proposed by earlier mechanistic and spectroscopic studies, under different potassium coverage.

Cyclic voltammograms were obtained in the presence of relevant concentrations of the different harmful gas components (NO, N_2O, SO_2 and H_2O) typically found in combustion exhausts, at 400 ° C and using a gas flowrate of 90 l h^{-1} (at 273 K and 1 atm). Gas Hourly Space Velocity during the measurements (calculated at 673 K and 1 atm and considering the bed volume occupied by the tubular electrochemical cell) was equal to 2921 h^{-1}.The potential was scanned between 4 V (starting potential) and – 3 V at a scan rate of 10 mV s^{-1} and current density (*j*) generated by the applied cyclic polarization was recorded as a function of the applied potential relative to the counter electrode.

Comparison of the cyclic voltammetric behaviour of the system under different gas atmospheres was carried out. With the exception of the experiments performed in the presence of SO_2, where voltammograms differed over the performed number of cycles, in all cases the compared voltammograms were obtained after no change with the number of cycles is observed.

On the other hand, the measurement of the open circuit potential by Solid Electrolyte Potentiometry (SEP) [2] under the different gaseous compositions tested, allowed obtaining useful information about the competitive adsorption of the different species present in the reaction ambient, anticipating or explaining the observed effect under each operating conditions and helping to elucidate the mechanism of adsorption, reaction, inhibition and poisoning over the catalyst-electrode. The cell was polarized at + 4 V for other 30 minutes before the open circuit potential measurements. The open circuit potential values were then

recorded over one hour aiming to ensure enough time for the de-polarization of the working electrode to be complete during the open circuit measurements. Measured open circuit potential corresponded to the steady state voltage value attained after one hour of testing, even though an almost stable value of open circuit potential was obtained after the first 30 minutes.

A summary of the feeding gas compositions employed is given in Table 1.

2. Results and Discussion

2.1 Solid Electrolyte Potentiometry (SEP) studies

In order to characterize the relative electropositive or electronegative nature of the different coexistent adsorbates, open circuit potential was measured under different gas atmospheres. The measured voltage represented the open circuit potential difference between the catalyst potential and that of the gold counter electrode, both exposed to the same gas atmosphere. It was observed that the presence of different adsorbed species on the catalyst surface modified the open circuit potential.

Chemisorption of an adsorbate on a metal gives rise to a real chemical bond, thus implying electron donation from adsorbate to metal or from metal to adsorbate. In the first case, the adsorbate is called electron donor (electropositive), whereas in the second, is called electron acceptor (electronegative). There is a certain scale of electronegativity or electron acceptor capacity, in which oxygen is one of the strongest electron acceptors. The adsorption of an electron acceptor (electronegative) increases the work function of the electrode, giving rise to higher values of the open circuit potential. On the contrary, the adsorption of electron donor (electropositive) species leads to a decline in the work function of the electrode, and therefore to low values of the open circuit potential. Moreover, on a potassium free catalyst surface

(unpromoted conditions) adsorption of electron donor adsorbates on active sites of the catalyst is favoured. With decreasing catalyst potential, the migration of promoter ions to the catalyst electrode is produced, hindering the adsorption of electron donor species and releasing the active sites, while favouring the adsorption of electron acceptor species [2].

Fig. 1 shows the effect of the addition of 500 ppm of N_2O, 109 ppm of SO_2, 492 ppm of NO or 10 % of H_2O to the standard gas (11.2 % CO_2, 4.7 % O_2, N_2 balance) on the difference in the measured open circuit potentials (ΔOCP) for the different gas atmospheres in relation to that of the standard gas (CO_2+O_2+ N_2) (as a measure of the change in the work function of the gas exposed Pt electrode surface), at 400 º C.

As can be observed in Fig. 1, the open circuit potential differences (ΔOCP) are actually small, with exception of the case of H_2O. This is considered to be due to the fact that the concentration of the different potential inhibitors and poisons (N_2O, SO_2 and NO) added to the standard gas is considerably smaller (hundreds of ppm) than that of CO_2 and O_2 (% v/v). On the contrary, the potential difference is high in the case of water because it is added in higher concentration (10 % v/v), comparable to that of CO_2 (11.2 %) and O_2 (4.7 %).

As can be observed in Fig. 1, N_2O is a somewhat stronger electron acceptor than CO_2, because the addition of N_2O slightly increases the value of open circuit potential in relation to that obtained under $CO_2/O_2/N_2$ (ΔOCP = +3 mV). As a result, N_2O adsorption is a little more favoured in the presence of potassium surface promoter, and under these conditions N_2O competes with CO_2 and O_2 for adsorption sites, i.e., a decrease in catalyst potential and, subsequently, an increase in the presence of surface promoter, is expected to favour the competitive adsorption of N_2O.

SO_2 is a bit weaker electron acceptor than CO_2, as can be derived from Fig. 1, because the addition of SO_2 to the standard gas composition results in a slightly lower open circuit potential vs. that obtained under standard gas (ΔOCP = -10 mV). Therefore, SO_2 could be

considered as an electron donor with respect to CO_2, and then on decreasing catalyst potential, i.e., on increasing the presence of surface promoter, SO_2 competitive adsorption and its potential poisoning effect are expected to be disfavoured.

NO is a bit stronger electron acceptor than CO_2, as can be derived from Fig. 1, since the addition of NO increases the value of open circuit potential in relation to that for the standard gas (ΔOCP = +42 mV). Therefore, CO_2 could be considered as an electron donor vs. NO, and as a result, on decreasing catalyst potential, CO_2 adsorption is hindered, while the competitive adsorption of NO is favoured.

As can be derived from Fig. 1, the addition of H_2O to the standard gas considerably increases the value of open circuit potential with respect to that for the standard gas (ΔOCP = +809 mV). According to literature [20], adsorption of H_2O on Pt was purely molecular resulting in a decrease of the work function, and, therefore of the measured open circuit potential. On the contrary, adsorption of H_2O on a K-covered Pt surface lead to H_2O dissociation and to the formation of adsorbed hydroxyl (OH) species with concomitant work function increase, resulting in a higher value of open circuit potential [20]. The amount of hydroxyl species formed was reported to be proportional to potassium coverage [20]. Given the increase in the value of the open circuit potential observed in the presence of water (ΔOCP= 809 mV), it can be concluded that water is adsorbed dissociatively on the catalyst surface, giving rise to formation of hydroxyl species, which are stronger electron acceptors than CO_2. Therefore, CO_2 could be considered as an electron donor vs. hydroxyl (OH) species, and as a result, with decreasing catalyst potential, migration of promoter ions to the Pt electrode occurs, displacing CO_2 from adsorption sites, while favouring the adsorption of OH (electron acceptor).

2.2 Cyclic voltammetry studies

2.2.1 Effect of O_2 on electropromoted CO_2 capture

In order to confirm the reported [12] effect of O_2 on electropromoted CO_2 capture under the specific operating conditions of this study, cyclic voltammetry experiments were firstly performed in the absence and in the presence of oxygen. Electropromoted adsorption/desorption cycles were obtained in the absence and in the presence of O_2 at 400 ºC. As can be observed in Fig. 2, in the presence of O_2, there was an increase in CO_2 adsorption capacity, i.e., in the amount of CO_2 captured via the carbonation process on passing from the first to the second cycle, being almost constant in successive cycles (steady state conditions), as can be deduced from the variation in the area (or θ_{KC1}) of the cathodic C1 peak over successive cycles in Fig. 2. This is probably due to the fact that the initial application of 4 V for 30 minutes apparently has not been sufficient to completely clean the Pt surface and therefore could exist some sites not available for CO_2 chemisorption, rendering C1 peak area lower in the first cycle. In fact, as cycling progresses, the cathodic peak near -1 V increases and slightly shifts toward more negative potentials

Fig. 3 compares cyclic voltammograms obtained in the absence and in the presence of O_2 at steady state conditions. The coverage of potassium (θ_K) on Pt calculated for the cathodic scan is also compared with that obtained for the anodic scan in the inset of Fig. 3. In both cases, the values of potassium coverage (θ_K) on Pt calculated for the cathodic and anodic scans are very similar (small differences could be ascribed to the error inherent to area integration). Therefore, a reversible promotional phenomenon was observed during cyclic voltammetry due to the formation (cathodic or negative current peaks) and decomposition (anodic or positive current peaks) of potassium surface compounds as a consequence of the negative (forward) and positive (backward) polarizations, respectively.

As can be observed in Fig. 3, for applied potential values higher than about 2.5 V, no cathodic (negative current) adsorption peaks appear in the forward scan. This means that under application of highly positive potentials, which allows maintaining the Pt surface free of electropositive ions [21–23], CO_2 does not chemisorb, only physisorbs weakly and molecularly at low temperature and desorbs without undergoing detectable dissociation at high temperature [19, 22, 24–26].

On the contrary, the presence of K on the Pt surface (Eq. 2) [21], as a result of electrochemical migration of potassium ions from the solid electrolyte to the catalyst surface under application of decreasing potentials, has been reported [24–25, 27] to promote CO_2 chemisorption and activation (Eq. 3), resulting in the formation of a highly distorted CO_2 molecule (CO_2^-) interacting strongly with the surface [21–22] and inducing the dissociation of CO_2, because of the caused strengthening of metal carbon bond and the weakening of C–O bond [22].

$$K^+(\beta\text{-}Al_2O_3) + e^- \rightarrow K\,(catalyst) \quad (2)$$

$$K + CO_2\,(g) \rightarrow K^+ \cdot\ CO_2^-\,(a) \quad (3)$$

In the absence of O_2, depending on the surface coverage of alkali metal (potassium in our case), CO_2^- may dissociate to CO, which could be adsorbed strongly on Pt leading to an inhibition of active sites, and O (a) (Eq. 4), at low potassium surface coverages or positive potentials [22, 24–25, 27], or be transformed into CO_3^{2-} and CO species (Eq. 5) [22, 27], at elevated potassium surface coverages or negative potentials.

$$CO_2^-\,(a) \rightarrow CO\,(a) + O^-\,(a) \quad (4)$$

$$2\ CO_2^-\,(a) \rightarrow CO\,(a) + CO_3^{2-}\,(a) \quad (5)$$

However, in the presence of O_2, at low potassium coverage, activated CO_2 (CO_2^-), which is formed on the catalyst surface, is stabilized, instead of being dissociated (in the absence of

O_2), giving rise to CO_3^{2-} (Eq. 6) [22, 27]. On the other hand, the presence of surface oxygen enhances the adsorption of background CO which reacts with excess oxygen to form CO_2 which desorbs easier [22, 27] and does not lead to inhibition of the active sites of Pt.

$$CO_2^- (a) + O^- (a) \rightarrow CO_3^{2-} (a) \quad (6)$$

The formation of C=O, carboxylate ion CO_2^-, chelating bidentate potassium carbonate and potassium bicarbonate has been previously confirmed by FTIR measurements during electropromoted propene combustion experiments at 350 ºC, over a similar Pt/K-β-Al_2O_3 catalyst [21]. The electrochemical system is also able to store CO_2, in the form of potassium carbonates, by adsorption over potassium sites electrochemically supplied to the catalyst surface [21, 23].

According to our previous study [12], in the absence of oxygen, the main current peak (C1), appearing at around – 1 V in the forward scans (Fig. 3), may be associated with the formation of potassium carbonate species, whereas the corresponding peak (A1), appearing at about 2 V in the backward scan, can be, therefore, attributed to the decomposition of these potassium compounds.

As can be observed also in Fig. 3, in the presence of oxygen two distinct cathodic current peaks, at about –1 V (C1) and –2 V (C2), appear during the cathodic (forward) potential scan. However, only one single anodic current peak, at about 1.5 V (A1+A2), is obtained during the anodic (backward) potential scan.

According also to our previous study [12], where the cyclic voltammetric behaviour of the system was also analysed the presence of O_2 only, in the presence of oxygen, the current peak (C2), appearing at around –2 V in the forward scan (Fig. 3), may be attributed to the formation of oxidic phases (potassium oxides and peroxides) resulting from the interaction between potassium ions and oxygen adsorbed on the catalyst surface during the electrochemical pumping of potassium ions, with the dominant product being K_2O (Eq. 7).

The reaction of a single oxygen atom with K_2O would lead to potassium peroxide, K_2O_2 (Eq. 8), which is reported to have a higher stability in the presence of excess oxygen compared to K_2O [28].

$$2\ K^+ + 2\,e^- + 1/2\,O_2 \rightarrow K_2O \quad (7)$$

$$K_2O + 1/2\ O_2 \rightarrow K_2O_2 \quad (8)$$

As can be observed in Fig. 3, both cathodic (negative current) peaks, C1 and C2, attributable to the formation of carbonate and oxidic species, respectively, appear during the forward (cathodic) scan. However, only an apparently single peak (A1 + A2) appears during the anodic (backward) polarization, which may be related, in accordance with our previous findings [12], with the decomposition of both potassium carbonate and oxidic species.

Starting from a potassium clean Pt surface (4 V) and on decreasing applied potential, during the cathodic (forward) scan, the adsorption of electron acceptor species, as O_2, is favoured [29] due to its higher electronegativity [30], increasing their surface coverage at the expense of electron-donors vs. O_2 (CO_2) and giving rise to a progressive increase in surface oxygen atoms formation by dissociative adsorption of O_2. According to our previous experimental findings [12], the peak which appeared in the cathodic scan at about – 1 V, could be also attributed to trapping of CO_2 as potassium carbonates (peak C1). It is sharper in the presence of oxygen (Fig. 3), i.e., the area (or θ_K) and height of the peak obtained under co-presence of CO_2 and O_2 are greater, probably, because, as indicated in the literature, in the absence of oxygen and at high cathodic (negative) voltages, which correspond to high K coverages, activated CO_2 (CO_2^-) is transformed into carbonate and CO (Eq. 5) [22, 27], while the presence of oxygen adatoms promotes bonding of CO_2 on potassium as carbonates and leads to its stabilisation (Eq. 6), instead to its disproportionation [22, 27], resulting in an increased carbonate formation, with respect to that in absence of oxygen, via electropromoted dissociative adsorption of O_2.

As can be observed in Fig. 3, in the presence of oxygen, another peak appears at approximately – 2 V (C2), which, in agreement with our previous experimental findings [12], could be also associated with the formation of more stable oxidic phases (Eqs. 7 and 8).

With increasing applied potential, and therefore decreasing K coverage, during the anodic (backward) potential scan, potassium ions are electrochemically removed from the Pt surface and returned to the solid electrolyte, allowing the decomposition of the CO_2 chemisorbed species or promoter compounds formed during the previous cathodic scan and, thus, the release of CO_2. As a consequence, an anodic peak appears, centred at about 1.5 V (A1+A2) which is considered [12] to be mainly due to the decomposition of carbonates formed by interaction of CO_2 with potassium ions electrochemically supplied to the catalyst electrode, although it also contains a contribution corresponding to the decomposition of the oxidic phases.

However, as can be deduced from Fig 3, in the absence of oxygen there was a difference between the area (or potassium surface coverage) of the cathodic C1 peak (carbonates) and the corresponding A1 peak, whereas in the presence of oxygen there was also a difference between the areas (or potassium surface coverage) of the sum of the C1 (carbonates) and C2 (oxides) cathodic peaks and the corresponding A1+A2 anodic peak. These differences are considered to be due to the formation of non-stable or non-electroactive chemisorbed CO_2 species (carboxylate ion, etc.) during the first part of the cathodic scan, which did not give rise to the appearance of a discernible/defined peak, but for which the corresponding CO_2 release by desorption or decomposition contributes to the A1 or A1+A2 area in the anodic scan.

As commented above, CO_2 is not chemisorbed on a "clean" Pt surface. On the contrary, in the presence of potassium CO_2 is initially chemisorbed as carboxylate ion (Eq. 3). However, at elevated potassium coverages and particularly in the presence of oxygen CO_2 is chemisorbed as CO_3^{2-} species via disproportion (Eq. 5) of carboxylate ion (in the absence of

O_2) or via surface reaction (Eq. 6) of carboxylate ion with oxygen adatoms resulting from electropromoted dissociative adsorption of oxygen (in the presence of O_2). Subsequent reaction of CO_3^{2-} species with potassium ions supplied via electrochemical pumping to the Pt surface may result in the formation of potassium carbonate species, i.e. potassium may act also as storage component. Therefore, at elevated potassium coverages, we can distinguish, in principle, two types of processes: the non-faradaic effect of promoter on the rate of CO_2 chemisorption as CO_3^{2-} species (Eq. 5 or 6) and formation of potassium carbonate species which may be limited only by the Faraday law (i.e., by the rate of ions supply).

The magnitude of electrochemical promotion is commonly described by the Faradaic efficiency Λ [2], defined as (Eq. 9):

$$\Lambda = \frac{r - ro}{I/F} = \frac{\Delta r}{I/F} \qquad (9)$$

where r is the electropromoted rate of chemisorbed CO_2 species formation and ro is the unpromoted rate (clean Pt surface, under application of 4 V), F is the Faradaic constant and I is the current. The term "I/F" corresponds to the rate of potassium ions supplied to catalyst according to the Faraday's law, whereas the term "Δr" corresponds to the electrochemically induced change in CO_2 chemisorption rate. Thus, $|\Lambda| = 1$ refers to pure Faradaic rate enhancement, and $|\Lambda| > 1$ implies electrochemical promotion.

Given that CO_2 is not chemisorbed on a "clean" Pt surface, i.e. the CO_2 chemisorption rate under unpromoted conditions is zero and that potassium is not a reactant in the chemisorption reaction (Eqs. 3 or 5 and 6), any positive potential-induced chemisorption rate change can be considered to be due to electrochemical promotion independently of the value of the Faradaic efficiency. However, in order to ascertain the non-Faradaicity of the electrochemical CO_2 adsorption, the Faradaic efficiency (Λ) has been calculated for the C1 peak in the presence of oxygen (where CO_2 capture as potassium carbonates is supposed to be

the highest), i.e., for the CO_2 chemisorption as CO_3^{2-} species (Eq. 6). The term I/F has been calculated from integration of the current density versus time for the peak C1 and the term Δr (equal to r) has been calculated from integration of the amount of adsorbed CO_2 (determined from NDIR analysis of the gas exiting the reactor) vs time curve (not shown) for the same time range. The resulted $|\Lambda|$ was equal to 3.6, i.e., higher than 1, indicating the non-Faradaicity of the CO_2 adsorption process.

2.2.2 Effect of H_2O on electropromoted CO_2 capture

In order to study the effect of H_2O on the behaviour of the catalyst towards the electropromoted CO_2 capture, cyclic voltammograms were also obtained in the presence of CO_2, O_2 and H_2O at 400 º C. Fig. 4 compares cyclic voltammograms obtained in the absence and in the presence of H_2O at steady state conditions. The values of potassium surface coverage (θ_K) calculated for the cathodic and anodic scans are shown in the inset of Fig. 4. Reversible electropromotion of the catalyst surface was also observed in the presence of water, given the good balance obtained between the cathodic and anodic processes.

As shown in Fig. 4, under the presence of CO_2, O_2 and H_2O, two cathodic peaks (C0 and C1) appear in the voltammogram. The C1 peak appears at a potential value very close to that obtained in $CO_2/O_2/N_2$ atmosphere (-1 V), therefore, it could be also attributed to the formation of potassium carbonate species. However, the area of C1 peak is lower in the presence of H_2O, resulting in a decreased carbonate formation ($\theta_K = 0.27$), with respect to that in absence of water ($\theta_K = 0.4$). The C_2 peak attributed to the formation of oxidic phases (potassium oxides and peroxides) disappeared in the presence of water. Instead a new peak (C0) appeared at about -0.5 V in the forward scan, which may be attributed to the formation

of potassium bicarbonate species by reaction between chemisorbed CO_2 and H_2O species [31].

An apparently single anodic (positive current) peak (A0+A1) is also observed in the presence of CO_2, O_2 and H_2O, which appears at a potential value (about 2 V) close to that obtained in the presence of CO_2 only (A1) (Fig. 3). The sum of the areas of cathodic peaks C0 ($\theta_K = 0.66$) and C1 ($\theta_K = 0.27$) almost matched the area of the A0+A1 ($\theta_K = 0.91$) anodic peak, suggesting that the latter is due to the decomposition of both carbonate and bicarbonate species previously formed by interaction between CO_2, O_2 and H_2O with potassium ions electrochemically supplied to the catalyst electrode. Therefore, in this case, a good agreement in calculated potassium surface coverage has been also obtained for the sum of C0 and C1 cathodic peaks and the corresponding A0+A1 anodic peak. The sum of the areas of peaks C0 ($\theta_K = 0.66$) and C1 ($\theta_K = 0.27$) obtained in the presence of water is higher than that of the C1 ($\theta_K = 0.4$) peak obtained in the absence of water, which seems to indicate that CO_2 capture capacity is enhanced in the presence of water by formation of potassium bicarbonate in addition to potassium carbonate species, avoiding, at the same time the formation of potassium oxidic species. The formation of the latter species could lead to deactivation of the system, since oxygen and water are believed to compete for the same adsorption sites at low potential values, given that both chemisorbed oxygen and water species (oxygen adatoms and hydroxyl groups, respectively) are considered to have a strong electron-accepting character [20].

According to literature [20, 32], adsorption of H_2O on clean Pt was purely molecular resulting in a decrease of the work function, and, therefore of the measured open circuit potential. On the contrary, adsorption of H_2O on a K-covered Pt surface is stronger and is accompanied by a large work function increase [20, 32], resulting in a higher value of open circuit potential. For low K coverages, H_2O adsorption was reported to be reversible [32],

whereas for K coverages above a critical value [32], adsorption of H_2O on K covered Pt leads to H_2O dissociation and to formation of hydroxyl (OH^-) species [32] which are also responsible for a work function increase [20], acting electronically as electron acceptors [33]. The amount of hydroxyl species formed was found to be proportional to potassium coverage [20]. Therefore, CO_2 could be considered as an electron donor vs. hydroxyl (OH^-) and as a result, CO_2 adsorption is preferentially favoured at low potassium coverage. In addition, hydroxyl groups generated are reported to destabilize K-CO_2 bond leading to a decrease in potassium carbonate formation that may explain the observed decrease in C1 peak in the presence of H_2O [34].

Starting from a potassium clean Pt surface (4 V) and with decreasing applied potential, during the cathodic (forward) scan, migration of K promoter ions to the Pt electrode occurs, favouring O_2 and H_2O dissociative adsorption. The interaction (Eqs. 6, 10 and 11) between chemisorbed CO_2, O_2 and H_2O species can result in the formation of potassium bicarbonates (Eq. 12) [32] and carbonates (Eq. 13) [22, 27], as indicated by the appearance of peaks C0 (at about -0.5 V) and C1 (around -1 V) in the cathodic scan.

$$CO_2\,(a) + H_2O\,(a) \rightarrow H^+\,(a) + HCO_3^-\,(a) \quad (10)$$

$$CO_3^{2-} + H^+\,(a) \rightarrow HCO_3^-\,(a) \quad (11)$$

$$2K^+\,(a) + 2HCO_3^-\,(a) \rightarrow 2KHCO_3\,(a) \quad (12)$$

$$2K^+\,(a) + CO_3^{2-}\,(a) \rightarrow K_2CO_3\,(a) \quad (13)$$

The C2 peak, attributed to the formation of oxidic phases (potassium oxides and peroxides) at high potassium surface coverages, does not appear in the presence of water. As commented above, the amount of surface hydroxyl species formed by H_2O dissociation increases with potassium coverage. Moreover, hydroxyl species, given their stronger electronegativity, may be preferentially adsorbed at low potential values (high K coverages), displacing oxygen from adsorption sites and avoiding the formation of oxidic phases. Moreover, it has been reported

that water may react with preadsorbed oxygen adatoms on Pt to form adsorbed hydroxyl groups (Eq. 14), which may limit also the formation of oxidic phases [35].

$$H_2O\,(a) + O\,(a) \rightarrow 2OH\,(a) \qquad (14)$$

Indeed, one can suggest that the chemical identity of potassium compounds could depend on the species more strongly adsorbed on the catalyst [16]. Taking into account the composition of the feed, the potassium compounds may be considered to be potassium carbonate and potassium bicarbonate. In fact, the presence of C=O, carbonaceous species, carboxylate-ion CO_2^-, chelating bidentate potassium carbonate and potassium bicarbonate were confirmed by FTIR measurements during electropromoted propene combustion experiments at 350 º C over a similar Pt/K-βAl_2O_3 system [21].

With increasing applied potential, and therefore decreasing K coverage, during the anodic (backward) potential scan, potassium ions are electrochemically removed from the Pt surface and returned to the solid electrolyte, allowing the decomposition of the promoter compounds formed during the previous cathodic scan and the release of CO_2. As a consequence, an anodic peak appears, centred at about 2 V (A0+A1) which is considered [21, 23] to be due to the decomposition of carbonates and bicarbonates formed by interaction of CO_2 with potassium ions electrochemically supplied to the catalyst electrode. In fact, the maximum decomposition rate of the stored potassium carbonate and bicarbonate species over similar Pt/K-βAl_2O_3 systems has been reported to be obtained at about 2 V [21, 23].

2.2.3 Effect of N_2O on electropromoted CO_2 capture

Fig. 5 compares cyclic voltammograms obtained in the absence and in the presence of N_2O at steady state conditions. The corresponding values of potassium surface coverage on Pt for both scans are shown in the inset of Fig. 5. Potassium surface coverage calculated for the

cathodic scan almost matches up with that obtained for the anodic scan, indicating that the electropromoted processes are also reversible in the presence of N_2O.

As shown in Fig. 5, in the presence of CO_2, O_2 and N_2O a cathodic shoulder (not well resolved) peak (SC1) appeared, at about -2 V, together with peak C1 in the forward scan. The C1 peak, corresponding to the formation of potassium carbonate species, appears at a potential value very close to that obtained in $CO_2/O_2/N_2$ atmosphere (-1 V), but the peak area is smaller in the presence of N_2O ($\theta_K = 0.29$), i.e., CO_2 capture through carbonate formation decreases in the presence of N_2O. It seems that, as reported in literature [36], N_2O species competitively adsorb onto the platinum sites (Eq. 15) preventing CO_2 adsorption and carbonate species formation, thus resulting in a decrease in the area of the peaks associated with carbonate formation (C1) and decomposition (A1). As can be observed in Fig. 1, N_2O is a somewhat stronger electron acceptor than CO_2, because the addition of N_2O slightly increases the value of open circuit potential in relation to that obtained under $CO_2/O_2/N_2$ (ΔOCP=3 mV). As a result, N_2O adsorption is a little more favoured in the presence of potassium surface promoter, and under these conditions competes with CO_2 and O_2 for adsorption sites, i.e., a decrease in catalyst potential and, subsequently, an increase in the presence of surface promoter, is expected to enhance the competitive adsorption of N_2O (Eq. 15), and therefore the associated inhibiting effect on CO_2 carbonation (Fig. 5).

$$N_2O\,(g) \rightarrow N_2O\,(a) \qquad (15)$$

The C2 peak attributed to the formation of oxidic phases (potassium oxides and peroxides) almost disappeared in the presence of N_2O. A new cathodic shoulder peak (SC1) appears at about -2 V in the cathodic scan which may be attributed, according to literature [37], to the formation of chemisorbed N_2O species (potassium nitrites and nitrates) by reaction (Eqs. 16-18) between adsorbed N_2O and surface oxygen adatoms resulting from by the dissociative adsorption of oxygen which is favoured at low potentials (high potassium coverage). The

resulting decrease in surface coverage of oxygen adatoms may limit the formation of oxidic phases (potassium oxides and superoxides), which may explain the disappearance of the C2 peak in the presence of N_2O.

$$N_2O\,(a) + O^-(a) \rightarrow NO + NO^-(a) \quad (16)$$

$$N_2O\,(a) + NO^-(a) \rightarrow N_2 + NO_2^-(a) \quad (17)$$

$$N_2O\,(a) + NO_2^-(a) \rightarrow N_2 + NO_3^-(a) \quad (18)$$

Regarding the backward scan, an additional anodic shoulder peak (SA1) appeared (at about 2.5 V), which may be ascribed to decomposition of promoter-derived nitrites/nitrates formed in the corresponding peak at – 2 V (SC1) during the previous cathodic polarization. In fact, the maximum decomposition rate of stored nitrate species over a similar Pt/K-βAl_2O_3 system has been reported to occur at about 3 V [3].

Therefore, it seems that N_2O species competitively adsorb onto the platinum sites preventing CO_2 adsorption and carbonate species formation.

As can be deduced from Fig. 5, in the presence of N_2O there was also a difference between the areas (or potassium surface coverage) of the sum of the C1 (carbonates) and C2 (oxides) cathodic peaks and the corresponding A1+A2 anodic peak. This difference may be again ascribed to the formation of non-stable or non-electroactive chemisorbed CO_2 species (carboxylate ion, etc.) during the first part of the cathodic scan, which did not give rise to the appearance of a discernible peak, but for which the corresponding CO_2 release by desorption or decomposition contributes to the A1+A2 area in the anodic scan.

In order to analyse the effect of the presence of N_2O on the electropromoted CO_2 capture performance of the catalyst, electropromoted adsorption/desorption cycles were also obtained in the presence of CO_2, O_2 and N_2O at 400 º C (Fig. 6). As can be observed in Fig. 6, the areas of C1 peaks obtained for the first and second cycle almost coincide; in addition, the areas of the A1 peaks obtained for the second and third cycle seem to coincide as well. Thus,

certain steady state can be observed, i.e., there was no poisoning effect of N_2O on CO_2 capture over Pt by N_2O derived compounds accumulation on the catalyst surface.

2.2.4 Effect of SO_2 on electropromoted CO_2 capture

Fig. 7 compares cyclic voltammograms obtained in the absence of SO_2 (at steady state conditions) and in the presence of SO_2 (3rd cycle, not at steady state conditions). As can be obtained from the values of potassium surface coverage obtained for each scan (inset of Fig. 7), in the presence of SO_2 there is also a good balance between the cathodic and anodic phenomena, confirming the reversibility of the electropromoted adsorption processes.

As shown in Fig. 7, in the presence of CO_2, O_2 and SO_2 an additional cathodic peak (SC0) appeared, at about open circuit conditions (0 V), together with peaks C1 and C2 in the forward (cathodic) scan. The C1 and C2 peaks, corresponding to the formation of potassium carbonate species and potassium oxidic species, respectively, appear at a potential values (-1 V and -2.2 V) very close to that obtained in $CO_2/O_2/N_2$ atmosphere, but the peak areas are smaller in the presence of SO_2, i.e., the formation of both potassium carbonate and oxidic species decreases in the presence of SO_2. Therefore, CO_2 capture was lower (θ_{KC1}=0.08) in the presence of SO_2, which demonstrates the negative effect of SO_2 on the CO_2 storing process. The other cathodic peak, SC0, is thought to be due to the formation of sulphur compounds (mainly potassium sulphites and sulphates). In fact, SO_2 is a potential poison of the electrocatalyst, because SO_2 can be adsorbed competitively on Pt sites [38] and under certain conditions, may be oxidized to SO_3 by reaction with chemisorbed oxygen [39-43] and can form quite stable sulphites/sulphates (Eqs. 19-23) [13, 44, 45]. The corresponding anodic peak (SA0) appearing in the backward scan at about 3 V, may be associated with the decomposition of sulphites and sulphates potentially formed in the forward scan. These

results show that the system is also able to store SO_2, likely as potassium sulphite and sulphate species [44, 46, 47].

$$SO_2\,(g) \Leftrightarrow SO_2\,(a) \quad (19)$$

$$1/2\,O_2\,(g) \Leftrightarrow O\,(a) \quad (20)$$

$$SO_2\,(a) + O\,(a) \Leftrightarrow SO_3\,(a) \quad (21)$$

$$SO_2\,(a) + O\,(a) + 2K\beta Al_2O_3 \rightarrow K_2SO_3 + 2K_2O\text{-deficient } K\beta Al_2O_3 \quad (22)$$

$$SO_3\,(a) + O\,(a) + 2K\beta Al_2O_3 \rightarrow K_2SO_4 + 2K_2O\text{-deficient } K\beta Al_2O_3 \quad (23)$$

SO_2 is a bit weaker electron acceptor than CO_2, as can be derived from Fig. 1, because the addition of SO_2 to the standard gas composition results in a slightly decrease of the open circuit potential (ΔOCP=-10 mV). Therefore, SO_2 could be considered as an electron donor vs. CO_2, and as a result, SO_2 adsorption is favoured in the absence of promoter, implying that, under unpromoted conditions (4 V), it would be preferentially adsorbed on the Pt surface, inhibiting CO_2 adsorption. Therefore, on decreasing catalyst potential and, then, increasing the presence of surface promoter, SO_2 adsorption is anticipated to decrease and adsorption sites become available for the CO_2 and O_2 chemisorption to take place [48]. At low potassium coverage, i.e. at low coverage of surface oxygen [48], the interaction between SO_2 and chemisorbed oxygen resulted in the formation of potassium sulphites/sulphates [13, 44], around 0 V (peak SC0 in Fig. 7) [38, 39, 41, 48]. A subsequent decrease in potential, i.e., a further increase in potassium promoter coverage, favoured CO_2 adsorption at the expense of that of SO_2, resulting in the formation of potassium carbonate species, which is maximum at about -1 V (peak C1 in Fig. 7). At very negative potentials, i.e., high potassium surface coverage, oxygen chemisorption is favoured resulting in the formation of potassium oxidic species (peak C2 in Fig. 7).

On the other hand, it can be observed that the maximum decomposition rate of the stored carbonates was obtained at about 1.5 V, whereas the maximum decomposition rate of

sulphite/sulphate species occurred at about 3 V. These results indicate that the sulphite (decomposition temperature: 497 ºC)/sulphate (decomposition temperature: 700 ºC) species exhibit a higher stability than the carbonates (decomposition temperature= 377 ºC) [49].

Therefore, the system is able to store both kinds of pollutants (CO_2 and SO_2) from the gas phase, and afterwards to electrochemically decompose them separately at different potentials, allowing selective separation of CO_2. In spite of the uncertainty related with the baseline to be used in the calculation of each peak area, a good agreement in calculated potassium surface coverage has been also obtained for each pair or combination of the corresponding peaks, i.e., the sum of C1 and C2 cathodic peaks and the A1+A2 anodic peak and the SCO and SAO peaks.

In order to ascertain the effect of SO_2 on the electropromoted CO_2 capture behaviour of the catalyst, electropromoted adsorption/desorption cycles were also carried out in the presence of CO_2, O_2 and SO_2 at 400 º C (Fig. 8).

SO_2 is competitively adsorbed onto the platinum sites, preventing CO_2 adsorption and carbonate species formation [45], and may be subsequently oxidised by oxygen adatoms deposited by dissociative adsorption of O_2 on Pt [39], giving rise to a decrease in potassium oxidic species formation and to poisoning of adsorption/storing sites through the formation of potassium sulphites and sulphates (Eqs. 22-23) [39,50]. This is revealed by the decrease in the area (or $\theta_{K)}$ of the peaks associated with carbonate (θ_{KC1} from 0.15 to 0.08, in the inset of Fig. 8) and oxidic species formation and decomposition (θ_{KA1+A2} from 0.17 to 0.08) and by the corresponding increase in the area of the peaks associated with sulphur species formation (SC0) and decomposition (SA0) (θ_K from 0.31 to 0.36), over successive cycles. This fact shows that there is a competition between SO_2 and CO_2 for adsorption on potassium storage sites which results in a decrease in the amount of K-based carbonate stored in the presence of SO_2 over successive cycles [47] and suggests that, in the presence of SO_2, CO_2 could be

eventually displaced from the surface (Eq. 24) [45, 49] and sulphur species could continue to accumulate. In fact, as can be observed in Fig. 8, as the cycling progresses the area, or equivalently θ_K (inset of Fig. 8) corresponding to the C1 peak decreases whereas those ascribed to SC0 peak increases, therefore, a deactivation process occurs that seems to involve oxidation of SO_2 to SO_3 over the metal component (Pt) followed by SO_3 adsorption on the storage component (K) [45].

$$K_2CO_3 + SO_2 + 1/2\,O_2 \rightarrow K_2SO_4 + CO_2 \quad (24)$$

2.2.5 Effect of NO on electropromoted CO_2 capture

Fig. 9 compares cyclic voltammograms obtained in the absence and in the presence of NO at steady state conditions. As can be deduced from the values of potassium surface coverage obtained for each scan (inset of Fig. 9), in the presence of NO, there is also a good balance between the cathodic and anodic phenomena, confirming the reversibility of the electropromoted adsorption processes. However, in this case, it was almost impossible to discern between the different peaks as a result of the distortion of the voltammogram induced by the presence of NO.

As shown in Fig. 9, in the presence of CO_2, O_2 and NO, a widening (probably due to the appearance of a second peak in both the cathodic and anodic regions) and an increasing intensity of the cathodic and anodic voltammetry peaks could be observed. This seems to indicate that additional surface species were formed during forward polarization, as indicated by the appearance of a cathodic shoulder peak at about – 2 V (SC1), which were decomposed during backward polarization giving rise to the corresponding anodic shoulder peak at about 2.5 V (SA1). In view of the reaction ambient, we could envisage that possible compounds formed could be potassium nitrite and nitrate phases. On the contrary, the C1 and C2 peaks, corresponding to the formation of potassium carbonate species and potassium oxidic species,

respectively, and the corresponding A1+A2 peak associated with their decomposition are unnoticeable in the presence of NO. These results seem to confirm that the system is also able to store NO, likely as potassium nitrite and nitrate species [51]. It has been previously reported [52] that, at 350 ºC and on a similar Pt/KBAl$_2$O$_3$ catalyst, NOx storage firstly proceeds with formation of nitrites. At temperatures above 200 ºC, the potassium nitrites, formed at the early stage of adsorption phase, can be oxidized into nitrates by oxygen atoms resulting from dissociative adsorption of O_2 on Pt [52, 53]. At saturation, only nitrates (bidentate and ionic nitrates) were detected to be present on the catalyst surface. A parallel pathway involving direct formation of nitrate species was also reported to be apparent [52].

NO is a bit stronger electron acceptor than CO_2, as can be derived from Fig. 1, since the addition of NO increases the value of open circuit potential in relation to that of the standard gas (ΔOCP = +42 mV). Therefore, CO_2 could be considered as an electron donor vs. NO and O_2 (which is one of the strongest electron acceptors), and as a result, CO_2 adsorption is favoured on a potassium free catalyst surface (unpromoted conditions). With decreasing catalyst potential during the forward scan, potassium ions migrate from the solid electrolyte to the catalyst electrode (Pt). According to the current rules of electrochemical promotion [2], the presence of an electropositive promoter (K+) on a catalyst film increases its ability to chemisorb electron acceptor species, in this case NO (Eq. 25) and O_2 (Eq. 20), disfavouring the chemisorption of electron donor ones (CO_2). The interaction between NO and oxygen chemisorbed species resulted in preferred formation of potassium nitrites/nitrates (shoulder peak SC1 in Fig. 9). The electrochemical addition of potassium ions to the Pt surface has been reported [3, 18, 23, 53] to promote NO oxidation reaction to NO_2 (Eq. 26), which has been identified as the rate determining step for the NOx storage process [3, 18, 23, 53–55]. The promotional effect of potassium was attributed to an increase in the O_2 adsorption rate, which has been identified as the rate-determining step of NO oxidation (Eq. 26) [53]. Thus the increase in the NO oxidation

reaction rate induced by the potassium ions initiated the NOx storage process. The next step is NO (Eq. 27) and NO_2 (Eq. 28) adsorption in the form of nitrites or nitrates [53–55]. Subsequently, potassium ions electrochemically pumped to the Pt catalyst active sites act as storage components and trap part of NO/NO_2 in the form of nitrites (Eq. 29)/nitrates (Eq. 30) [16, 17, 53, 56–59] . Therefore, one can distinguish two types of processes: the non-faradaic effect of promoter on the NO oxidation rate and the formation of potassium nitrates species limited by the Faraday law (i.e., by the rate of ions supply) [3].

$$NO(g) \Leftrightarrow NO(a) \quad (25)$$

$$NO(a) + O(a) \Leftrightarrow NO_2(a) \quad (26)$$

$$NO(a) + O^-(a) \rightarrow NO_2^-(a) \quad (27)$$

$$NO_2(a) + O^-(a) \rightarrow NO_3^-(a) \quad (28)$$

$$NO_2^-(a) + K^+(a) \rightarrow KNO_2 \quad (29)$$

$$NO_3^-(a) + K^+(a) \rightarrow KNO_3 \quad (30)$$

On the other hand the removal of potassium ions from the catalyst surface during the backward scan allows the decomposition of the previously stored phases [3, 56], which leads to the observed anodic shoulder peak (SA1).

In order to determine the effect of NO on the electropromoted CO_2 capture behaviour of the catalyst, electropromoted adsorption/desorption cycles were also performed in the presence of CO_2, O_2 and NO at 400 º C (Fig. 10).

As can be observed in Fig. 10, in the presence of NO, the cathodic C1 and C2 peaks and the anodic peak (A1+A2) related to formation and decomposition of potassium carbonate and oxide species are unnoticeable along cycles, which demonstrates the strong detrimental effect of NO on the CO_2 storing process. It can be also observed that the maximum decomposition rate of the nitrate species occurred at about 2.5 V, indicating that the nitrate species have a higher stability

than the carbonates (maximum decomposition rate at about 1.5 V). Carbonates are stable between 200-650 K. Carbonates decomposition start at temperatures above 650 K and is completed above 800 K [27]. In addition, stability of potentially formed potassium carbonates is also lower at higher temperatures [60, 61]. Potassium carbonate and bicarbonate have been reported to be decomposed under application of 2 V, whereas decomposition of the nitrate species occurred at 3 V [21, 23]. At high temperature (usually T> 400 º C), the NOx storage is limited by the stability of adsorbed species [23, 60], whereas at low temperature (usually T<250 ºC) it is limited by the low NO oxidation rate [3, 53].

Therefore, it seems that there is a competition between NO and CO_2 for adsorption on electrochemically supplied alkali metal (potassium) storage sites [3, 23, 24, 26, 34, 62, 63] which results in a strong decrease in the amount of K-based carbonates stored in the presence of NO and suggests that, in the presence of NO, CO_2 is displaced from the surface and nitrate species could quickly accumulate on the catalyst surface, because, as can be observed in Fig.10, a steady state behaviour seems to be attained from the second cycle, given that voltammograms for the second and third cycles almost coincide. In fact, according to literature, alkali metal carbonates can be converted into alkali metal nitrates depending on operating conditions [64], as a result of the progressive decomposition of surface carbonates upon NOx uptake according to the stoichiometry of reaction (Eq. 31) [40, 56, 64, 65]. It has been previously observed that, at 300 ºC, NOx can replace all carbonates and carboxylates in the alkali metal phase in the absence of CO_2 [49, 64, 65], whereas in the presence of CO_2 in the feed, not all the alkali metal carbonates can be converted into alkali metal nitrates [66] and, even, CO_2 may induce nitrate decomposition and NOx release, due to the formation of stable alkali metal carbonates [66, 67]. Moreover, according to literature, the stability of these species (nitrates and carbonates), relative to each other, differs depending on reaction conditions [24, 68]. Some authors reported that the inhibiting effect of NOx on CO_2 adsorption over electrochemically supplied potassium storing

sites decreased at higher temperature because the stability of carbonates compared to the respective nitrates increases with temperature [24, 68].

It has been reported [23] that the ability of Pt to catalyse NO to NO_2 does not drive off adsorbed carboxylates, but instead its ability to catalyse adsorbed NO_2 to an adsorbed nitrate is responsible for this destabilization, i.e., the presence of Pt contributes to the destabilization of the K-CO_2- bonds, allowing additional nitrate formation [34].

$$K_2CO_3 + 2\,NO + 3/2\,O_2 \rightarrow 2KNO_3 + CO_2 \quad (31)$$

2.3 Catalyst characterisation studies

XRD spectra of fresh (as prepared) and used (after exposure to reaction conditions) samples of Pt catalyst-working electrode film are compared in Fig. 11. The peaks at 2θ about 39.7º, 46.2º, 67.4º, 81.2º and 85.7º were identified as the typical diffraction peaks of Pt metal (JCPDS card no. 98-064-9494), whereas the remaining peaks were assigned to the K-βAl_2O_3 solid electrolyte (JCPDS card no. 98-020-0993 and 98-020-1094). No peaks of platinum oxide, or other phases, were detected for the samples both as prepared and after testing,

As can be deduced by XRD analysis (Fig. 11), it seems that exposure of the Pt catalyst film to the testing gas environment resulted in sintering of the Pt particles, giving rise to an increase in crystallinity, as revealed by the fact that typical XRD peaks of metallic Pt exhibited higher intensity in the used sample.

As can be observed also in Fig. 11, the intensities of XRD peaks related to K-βAl_2O_3 also increased in the used samples. This increase is considered to be due to hydrothermal sintering of Al_2O_3, which is typical to occur in the presence of high water concentrations (10 % in our case) and which is accelerated by temperature (400 ºC).

In order to evaluate the nature of the different species which were expected to have been accumulated on the Pt surface, the sample used in multi-cycle tests under different gas composition was characterised by XPS. A fresh sample was also analysed in order to provide an initial reference state for the material.

The XPS analysis of the fresh (as deposited) sample seems to indicate that Pt is mainly present as metal, as suggested by the appearance of a peak at a binding energy of about 70.9 eV [69], in the Pt $4f_{7/2}$ spectra.

The XPS spectra of the used (after testing) sample revealed the presence of additional superficial compounds that could not be identified by XRD, resulting in Pt being present as Pt oxides (6.5 %) and hydroxides (30.1 %), which may be formed upon exposure of the Pt film to wet and/or oxidant testing gas environments, in addition to metallic Pt (63.5 %), as revealed by the appearance of peaks at binding energies of about 74 and 72/74.4 eV [70–72], respectively, in the Pt $4f_{7/2}$ spectra. These results suggest that the Pt film could be partially oxidized/hydroxylated under reaction gas environment.

XPS results seem to confirm the partial hydrothermal sintering of K-βAl_2O_3 by the appearance of a peak at a binding energy of about 119 eV in the Al 2s XPS spectra of the used sample, associated with the formation of $Al(OH)_3$ [73].

XPS results seem to provide insights of certain accumulation of sulphur and nitrogen species on the Pt surface.

The presence of peaks at binding energies of about 164 [70] and 168.12 eV [74] in the S $2p_{3/2}$ spectra may be indicative of some formation of sulphite (31.5 %) and sulphate (68.5 %) species, respectively, on the Pt surface, which could contribute also to the decrease in CO_2 capture over successive cycles, observed in the tests performed in the presence of SO_2. This is accompanied by the appearance of a peak (at 533.6 eV) in the O 1s region that could be ascribable also to the formation of sulphate species [75].

There are also signs of nitrogen accumulation on the Pt surface, as indicated by the appearance of peaks at about 399.2 [70], 400.5 [76] and 402 [71] eV in the N 1s spectra of the used sample which could be attributed to the presence of nitrite, adsorbed NOx and nitrate surface species, respectively.

Therefore, results of catalyst characterization, before and after the tests, seem to confirm the assumed identity of phases proposed by earlier mechanistic and spectroscopic studies reported in literature, because XPS results reveal that Pt could be partially oxidized /hydroxylated under reaction gas environment, given that the presence of Pt oxides and hydroxides on the surface of the used sample was confirmed by the appearance of XPS peaks attributable to these compounds. XPS has also revealed the presence of nitrite, adsorbed NOx, nitrate, sulphite and sulphate surface species in the used Pt catalyst. However, there were no XPS or XRD results which could suggest the possible formation of potassium compounds on the K-β-Al_2O_3 electrolyte surface.

3. Conclusions

Cyclic electropromoted CO_2 capture studies showed that the tubular Pt/K-βAl_2O_3 system is able to capture CO_2 under conditions representative of combustion flue gases at bench scale, not only by selective electropromoted adsorption but also in the form of carbonates and bicarbonates by reaction with potassium ions electrochemically supplied to Pt surface. CO_2 capture is enhanced in the presence of O_2 and H_2O. The CO_2 capture behaviour of the system is almost unaffected by the presence of N_2O. SO_2 poisons CO_2 capture, whereas the presence of NO appears to considerably hinder CO_2 capture. The Pt/K-βAl_2O_3 system can be regenerated, allowing CO_2 separation, by electrochemical decomposition of previously stored compounds at different potentials without increasing temperature, with consequent energy

saving. Electrochemical promotion seems to be a promising technique to diminish the inhibiting or poisoning effect of the different harmful exhaust gas components, because it allows decreasing of their competitive adsorption by modification of surface potassium coverage through variation of the applied potential.

Acknowledgements

The authors acknowledge support from Ministerio de Ciencia e Innovación of Spain (Project ENE2010-15569). Pedro J. Martínez is grateful to Ministerio de Ciencia e Innovación of Spain for the research grant BES-2011-046902.

References

[1] C. Song, Catal. Today 115 (2006) 2.

[2] C. G. Vayenas, S. Bebelis, C. Pliangos, S. Brosda, D. Tsiplakides, "Electrochemical Activation of Catalysis: Promotion, Electrochemical Promotion and Metal-Support Interactions", Kluwer Academic/Plenum Publishers, New York, 2001.

[3] A. de Lucas-Consuegra, A. Caravaca, M. J. Martín de Vidales, F. Dorado, S. Balomenou, D. Tsiplakides, P. Vernoux, J. L. Valverde, Catal. Commun. 11 (2009) 247.

[4] M.C. Stern, F. Simeon, T. Hammer, H. Landes, H.J. Herzog, T.A. Hatton, Energy Procedia 4 (2011) 860.

[5] H. W. Pennline, E. J. Granite, D. R. Luebke, J. R. Kitchin, J. Landon, L. M. Weiland, Fuel 89 (2010) 1307.

[6] N. Kotsionopoulos, S. Bebelis, J. Appl. Electrochem. 40 (2010) 1883.

[7] D. Tsiplakides, S. Balomenou, Cat. Today 146 (2009) 312.

[8] T. Chao, K. J. Walsh, P. Fedkiw, Solid State Ionics 47 (1991) 277.

[9] L. Bultel, C. Roux, E. Siebert, P. Vernoux, F. Gaillard, Solid State Ionics 166 (2004) 183.

[10] C.G. Vayenas, A. Ioannides, S. Bebelis, J. Catal 129 (1991) 67.

[11] J. Yi, A. Kaloyannis, C.G. Vayenas, Electrochimica Acta 38 (1993) 2533.

[12] E. Ruiz, D. Cillero, A. Morales, G. San Vicente, G. de Diego, P. J. Martínez, J.M. Sánchez, Electrochimica Acta 112 (2013) 967.

[13] E.I. Papaioannou, S. Souentie, A. Hammad, C.G. Vayenas, Catal. Today 146 (2009) 336.

[14] E. Ruiz, D. Cillero, P.J. Martínez, A. Morales, G. San Vicente, G. de Diego, J.M. Sánchez, Catal. Today 210 (2012) 55.

[15] A. Morales, EU EP 1 321 539 A2.

[16] F. Dorado, A. de Lucas-Consuegra, P. Vernoux, J.L. Valverde, Appl. Catal., B 73 (2007) 42.

[17] F. Dorado, A. de Lucas-Consuegra, C. Jiménez, J.L. Valverde, Appl. Catal., A 321 (2007) 86.

[18] A. de Lucas-Consuegra, F. Dorado, J.L. Valverde, R. Karoum, P. Vernoux, Catal. Commun. 9 (2008) 18.

[19] P. Vernoux, F. Gaillard, C. Lopez, E. Siebert, Solid State Ionics 175 (2004) 609.

[20] M. Kiskinova, G. Pirug, H.P. Bonzei, Surf. Sci. 150 (1985) 319.

[21] A. de Lucas-Consuegra, F. Dorado, J.L. Valverde, R. Karoum, P. Vernoux, J. Catal. 251 (2007) 474.

[22] Z. M. Liu, Y. Zhou, F. Solymosi, J. M. White, Surf. Sci. 245 (1991) 289.

[23] L.V. Mattos, E.R. Oliveira, P.D. Resende, F.B. Noronha, F.B. Passos, Catal. Today 77 (2002) 245.

[24] E.C. Corbos, X. Courtois, N. Bion, P. Marecot, D. Duprez, Appl. Catal. B 76 (2007) 357.

[25] J.M. Ricart, M.P. Habas, A. Clotet, D. Curulla, F. Illas, Surf. Sci. 460 (2000) 170.

[26] I. Nova, L. Castoldi, L. Lietti, E. Tronconi, P. Forzatti, Catal. Today 75 (2002) 431.

[27] M. Xin, I.C. Hwang, S.I. Woo, Catal. Today 38 (1997) 187.

[28] T.J. Toops, D.B. Smith, W.P. Partridge, Catal. Today 114 (2006) 112.

[29] S. Brosda, C.G. Vayenas, J. Wei, Appl. Catal. B 68 (2006) 109.

[30] F.J. Willians, M.S. Tikhov, A. Palermo, N. Macleod, R.M. Lambert, J. Phys. Chem. B 105 (2001) 2800.

[31] B.T. Zhang, M. Fan, A.E. Bland, Energy & Fuels 25 (2011) 1919.

[32] H.P. Bonzel, G. Pirug, Physical Review Letters 58 (1987) 20.

[33] A.P. Seitsonen, Y. Zhu, K. Bedürftig, H. Over, J. Am. Chem. Soc. 123 (2001) 7347.

[34] T.J. Toops, D.B. Smith, W.S. Epling, J.E. Parks, W.P. Partridge, Appl. Catal. B 58 (2005) 255.

[35] W. Lew, M.C. Crowe, C.T. Campbell, J. Carrasco, A. Michaelides, J. Phys. Chem. C 115 (2011) 23008.

[36] M. Konsolakis, C. Drosou, I.V. Yentekakis, Appl. Catal., B 123-124 (2012) 405.

[37] C. Sang, C.R.F. Lund, Catal. Lett. 73 (2001) 73.

[38] J. Zhai, M. Hou, D. Liang, Z. Shao, B. Yi, Electrochemistry Communications 18 (2012) 131.

[39] A. Hammad, S. Souentie, E.I. Papaioannou, S. Balomenou, D. Tsiplakides, J.C. Figueroa, C. Cavalca, C.J. Pereira, Appl. Catal. B 103 (2011) 336.

[40] J. Dawody, M. Skoglundh, L. Olsson, E. Fridell, Appl. Catal. B 70 (2007) 179.

[41] C. Quijada, A. Rodes, J.L. Vázquez, J.M. Pérez, A. Aldaz, Journal of Electroanalytical Chemistry 394 (1995) 217.

[42] P.H. Yang, J.H. Yang, C.S. Chen, D.K. Peng, G.Y. Meng, Solid State Ionics 86-88 (1996) 1095.

[43] Y.W. Lee, J.W. Park, J.H. Choung, D.K. Choi, Environ. Sci. Technol. 36 (2002) 1086.

[44] G. Jasinki, P. Jasinki, B. chaculski, A. Novakowski, Materials-Science-Poland 24 (2006) 265.

[45] J.A. Anderson, Z. Liu, M. Fernández García, Catal. Today 113 (2006) 25.

[46] T.J. Toops, J.A. Pihl, Catal. Today 136 (2008) 164.

[47] E. Schreier, R. Eckelt, M. Richter, R. Fricke, Appl. Catal. B 65 (2006) 249.

[48] F. Xu, R. Xu, S. Mu, Electrochimica Acta 112 (2013) 304.

[49] L. Wang, H. Zhou, K. Liu, Y. Wu, L. Dai, R.V. Kumar, Solid State Ionics 179 (2008) 1662.

[50] N. Rao, C.M. van den Bleek, J. Schoonman, Solid State Ionics 53-56 (1992) 38.

[51] D. Uy, K.A. Wiegand, A.E. O'Neill, M.A. Dearth, W.H. Weber, J. Phys. Chem. B 106 (2002) 387.

[52] L. Castoldi, L. Lietti, P. Forzatti, S. Morandi, G. Ghiotti, F. Vindigni, J. Catal. 276 (2010) 335.

[53] A. de Lucas-Consuegra, A. Caravaca, P. Sánchez, F. Dorado, J.L. Valverde, J. Catal. 259 (2008) 54.

[54] X. Li, P. Vernoux, Appl. Catal. B: Environ. 61 (2005) 267.

[55] S. Hammache, LI.R. Evans, E.N. Coker, J.E. Miller, Appl. Catal. B: Environ. 78 (2008) 315.

[56] R. Matarrese, L. Castoldi, N. Artioli, E. Finocchio, G. Busca, L. Lietti Appl. Catal. B: Environ. 144 (2014) 783.

[57] M. Konsolakis, I.V. Yentekakis, Appl. Catal. B: Environ. 29 (2001) 103.

[58] A. de Lucas-Consuegra, A. Caravaca, F. Dorado, J.L. Valverde, Catal. Today 146 (2009) 330.

[59] I.V. Yentekakis, V. Tellou, G. Botzolaki, I.A. Rapakousios, Appl. Catal. B: Environ. 56 (2005) 229.

[60] A. Kotsifa, D.I. Kondarides, X.E. Verykios, Appl. Catal. B: Environ. 72 (2007) 136.

[61] Y. Chi, S.S.C. Chuang, Catalysis Today 62 (2000) 303.

[62] E.C. Corbos, X. Courtois, F. Can, P. Marecot, D. Duprez, Appl. Catal. B: Environ. 84 (2008) 514.

[63] C.M.L. Scholz, V.R. Gangwal, M.H.J.M. de Croon, J.C. Schouten, Appl. Catal. B: Environ. 71 (2007) 143.

[64] H. Mahzoul, J.F. Brilhac, P. Gilot, Appl. Catal. B: Environ. 20 (1999) 47.

[65] T. Lesage, J. Saussey, S. Malo, M. Hervieu, C. Hedouin, G. Blanchard, M. Daturi,

[66] J.-Y. Luo, W.S. Epling, Appl. Catal. B: Environ. 97 (2010) 236.

[67] A. Lindholm, N.W. Currier, E. Fridell, A. Yezerets, L. Olsson, Appl. Catal. B: Environ. 75 (2007) 78.

[68] W.S. Epling, J.E. Parks, G.C. Campbell, A. Yezerets, N.W. Currier, L.E. Campbell, Catalysis Today 96 (2004) 21.

[69] A. Mosquera, D. Horwat, L. Vazquez, A. Gutierrez, A. Erko, A. Anders, J. Andersson, J.L. Endrino, J. Mater. Res. 27 (2012) 829.

[70] C.D. Wagner, W.M. Riggs, L.E. Davis, J.F. Moulder, "Handbook of X-ray photoelectron spectroscopy", Perking-Elmer Corp., Eden Prairie, 1979.

[71] D. Briggs, M.P. Seah, "Practical Surface Analysis Volume 1: Auger and X-ray Photoelectron Spectroscopy 2nd Edn", John Wiley & Sons, New York, 1990.

[72] T.L. Barr, Journal of Physical Chemistry 82 (1978) 1801.

[73] J.A. Rotole, P.M.A. Sherwood, Surface Science Spectra 5 (1998) 32.

[74] R.A. Walton, Coordination Chemistry Reviews 31 (1980) 183.

[75] P. de Donato, C. Mustin, R. Benoit, R. Erre, Applied Surface Science 68 (1993) 81.

[76] X. Gao, P. Chen, J. Liu, Materials Letters 65 (2011) 685.

Figure Captions

Fig. 1. Effect of the addition of 500 ppm of N_2O, 109 ppm of SO_2, 492 ppm of NO or 10 % of H_2O to the standard gas (11.2 % CO_2, 4.7 % O_2, N_2 balance) on the difference (ΔOCP) between the measured open circuit potentials for the different gas atmospheres and that for the standard gas (CO_2+O_2+ N_2) at 400 º C .

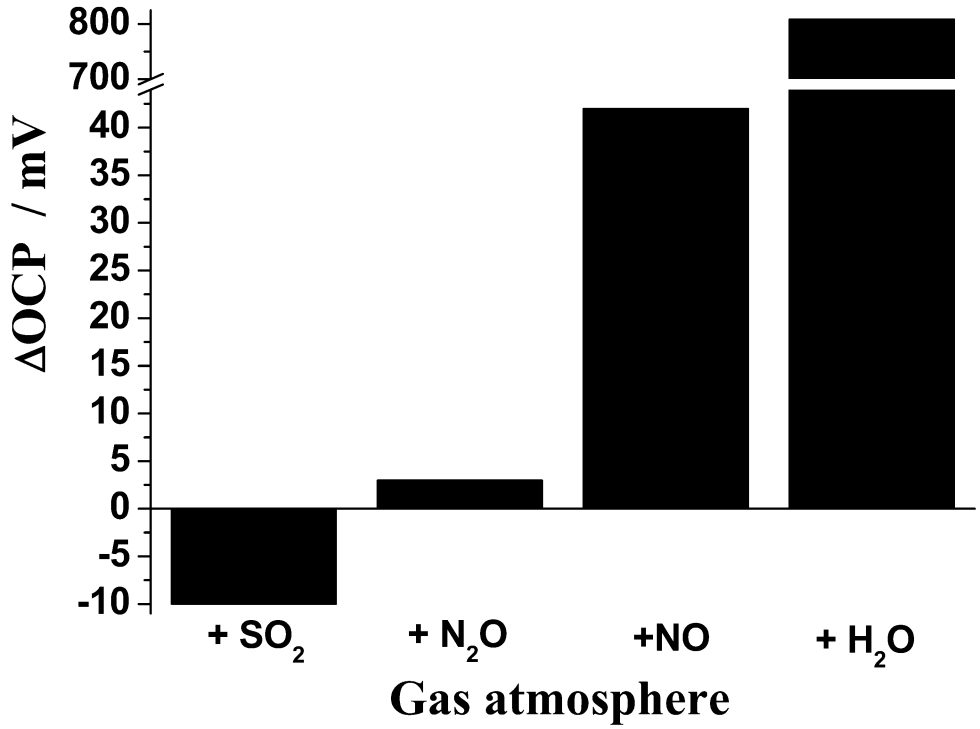

Fig. 2. Cyclic voltammograms recorded over Pt/K-βAl_2O_3 in the presence of CO_2 (11.2 %) and O_2 (4.7 %) at 400 ° C: 1st cycle (black), 2nd cycle (red), 3rd cycle (blue). Inset: Potassium surface coverage corresponding to the cathodic C1 peak (carbonate formation) over cycles.

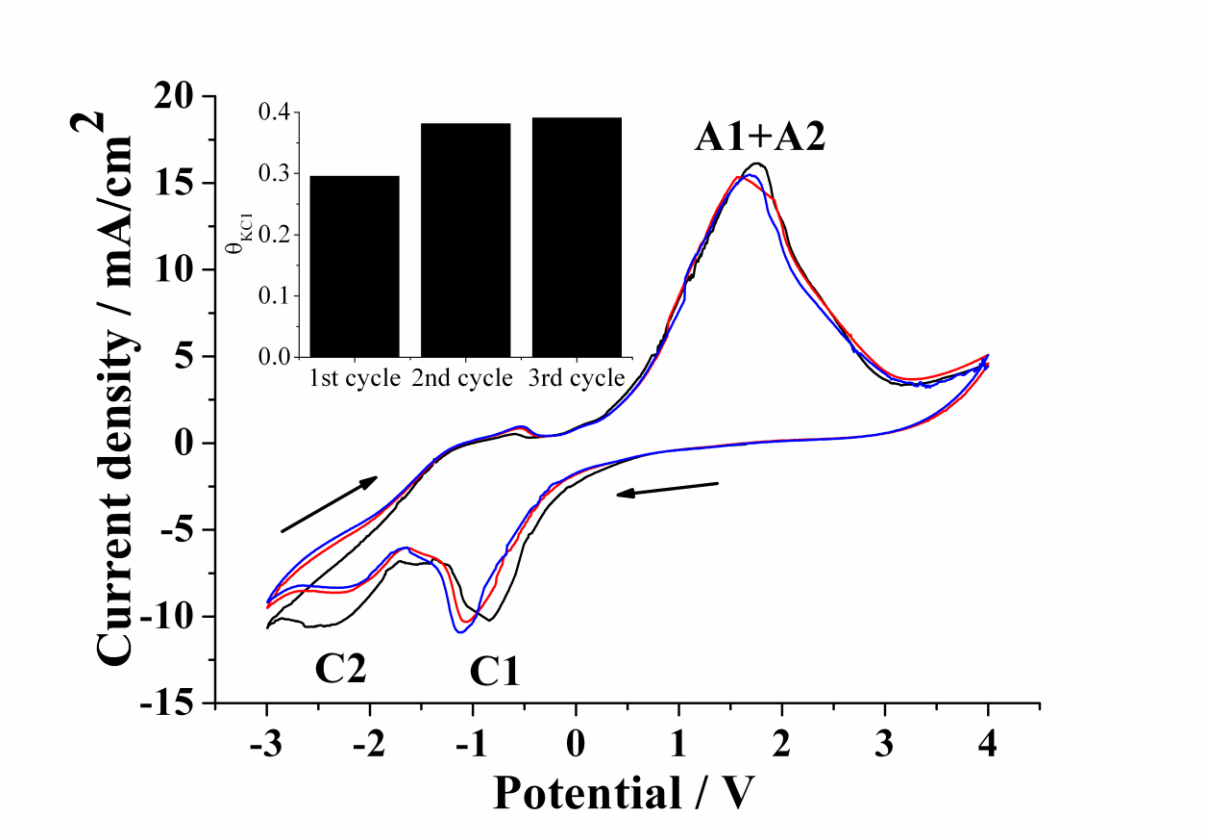

Fig. 3. Effect of O_2 on electropromoted CO_2 capture over Pt/K-βAl_2O_3. Cyclic voltammograms recorded at 400 ºC and under different gas compositions: 11.2 % CO_2 in N_2 (black), 11.2 % CO_2 and 4.7 % O_2 in N_2 (red). Inset: Potassium surface coverage for the cathodic and anodic scans under different gas compositions.

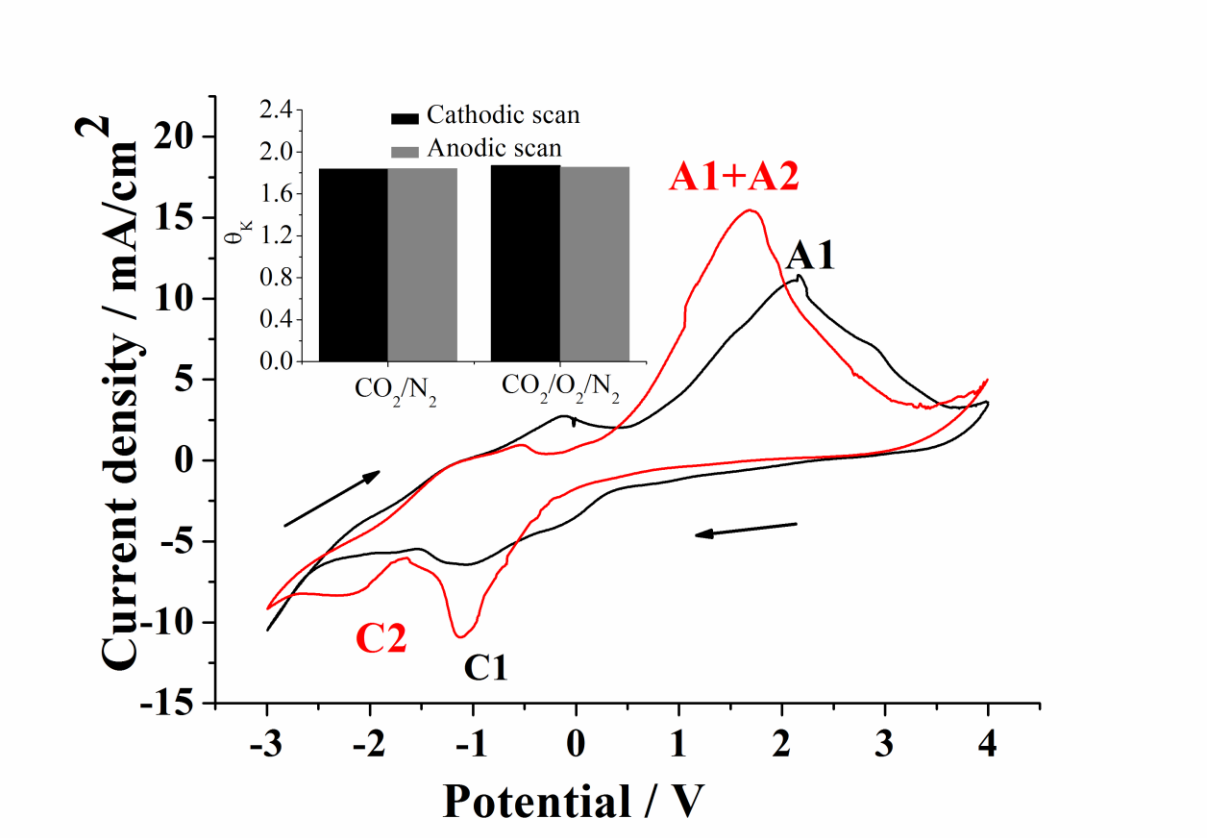

Fig. 4. Effect of H_2O on electropromoted CO_2 capture over Pt/K-βAl_2O_3. Cyclic voltammograms recorded at 400 ºC and under different gas compositions: 11.2 % CO_2, 4.7 % O_2 and 10 % H_2O in N_2 (black), 11.2 % CO_2 and 4.7 % O_2 in N_2 (red). Inset: Potassium surface coverage for the cathodic and anodic scans under different gas compositions.

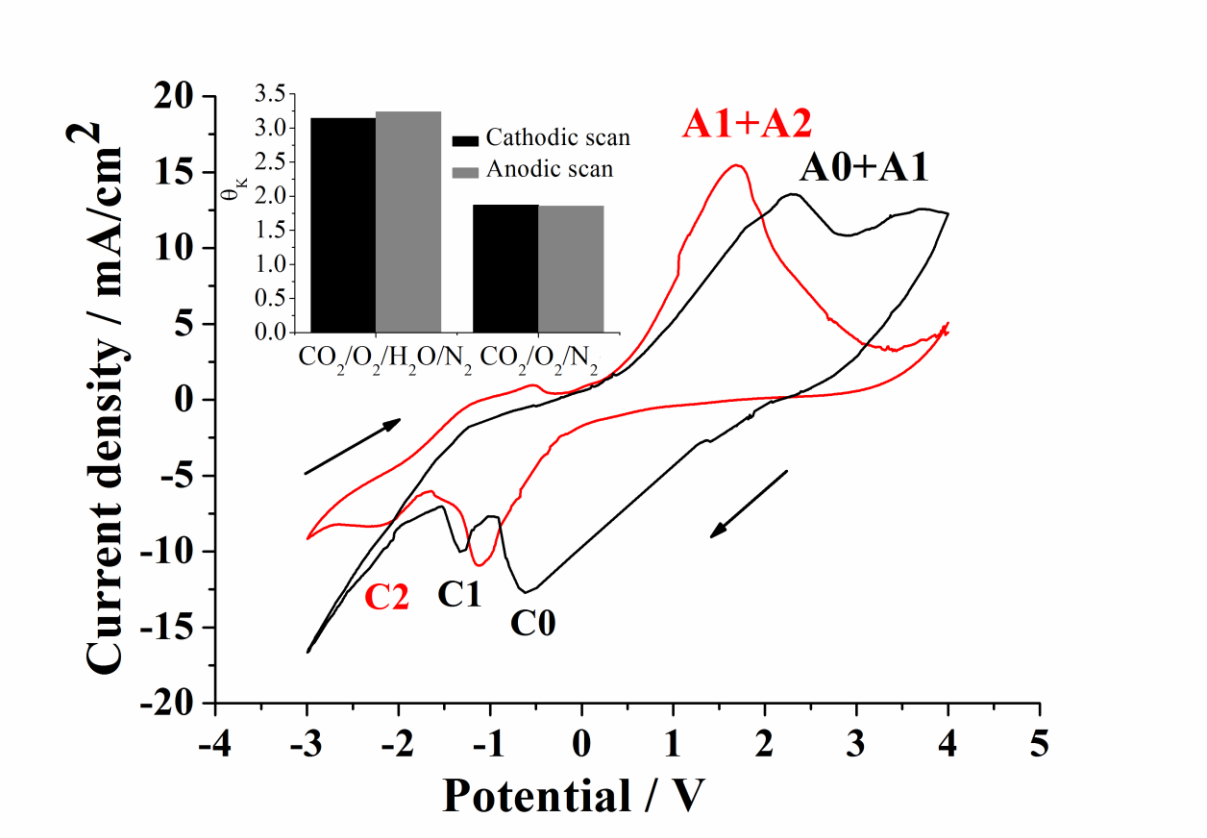

Fig. 5. Effect of N_2O on electropromoted CO_2 capture over Pt/K-βAl_2O_3. Cyclic voltammograms recorded at 400 ºC and under different gas compositions: 11.2 % CO_2, 4.7 % O_2 and 500 ppm N_2O in N_2 (black), 11.2 % CO_2 and 4.7 % O_2 in N_2 (red). Inset: Potassium surface coverage for the cathodic and anodic scans under different gas compositions.

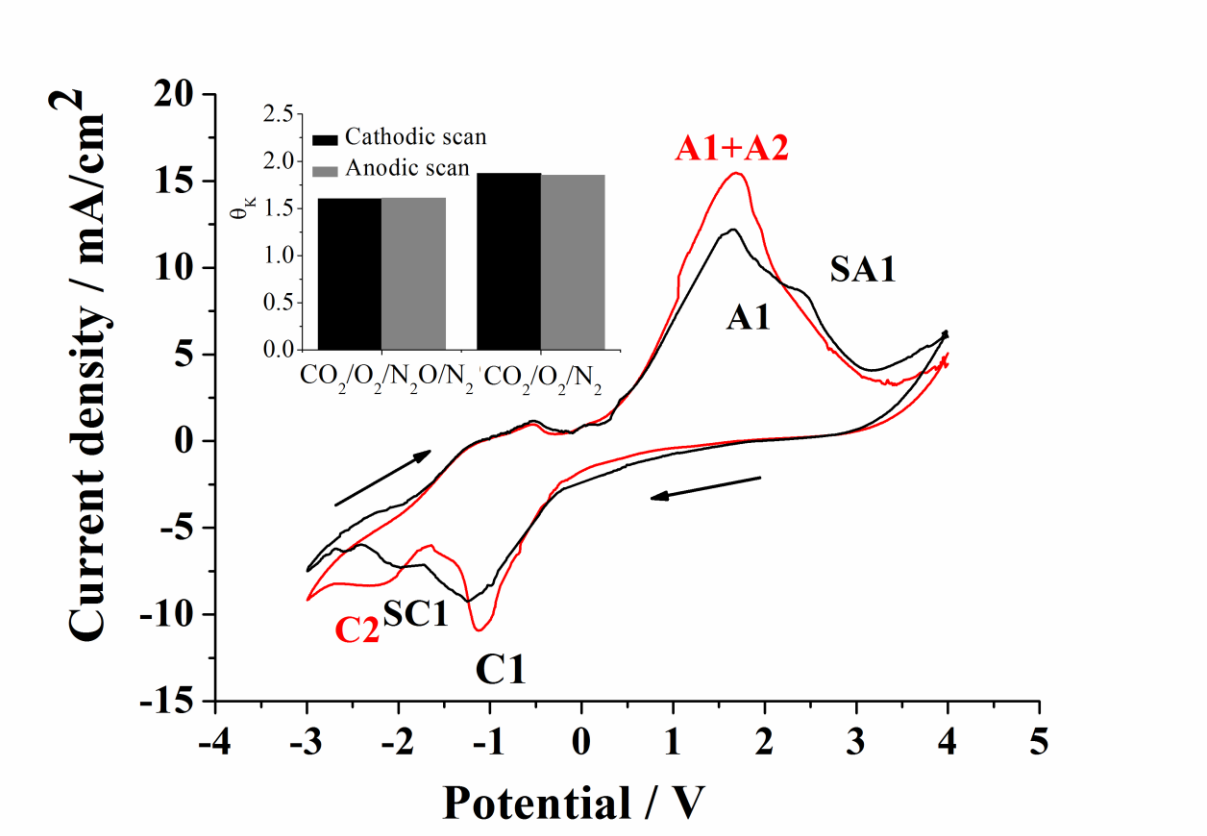

Fig. 6. Cyclic voltammograms recorded over Pt/K-βAl_2O_3 in the presence of CO_2 (11.2 %), O_2 (4.7 %) and N_2O (500 ppm) at 400 ° C: 1st cycle (black), 2nd cycle (red), 3rd cycle (blue).

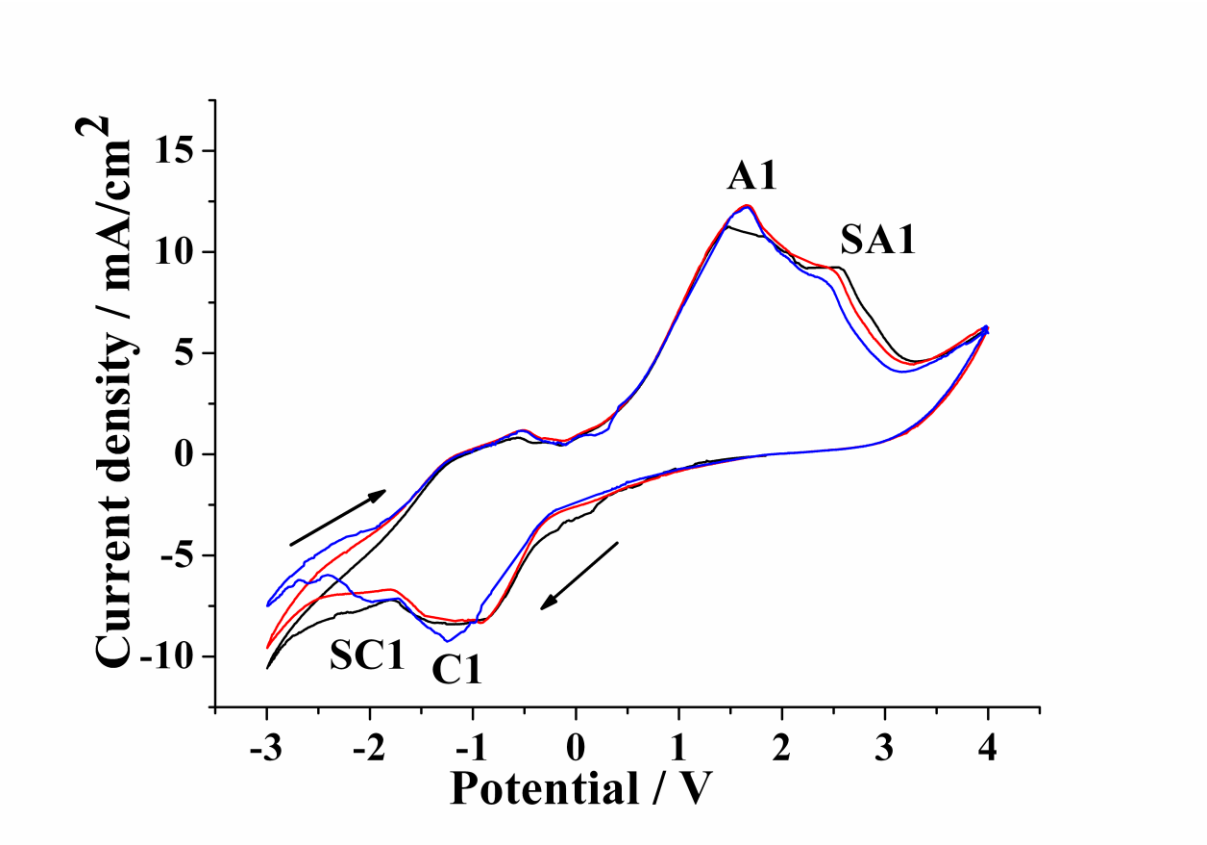

Fig. 7. Effect of SO_2 on electropromoted CO_2 capture over Pt/K-βAl_2O_3. Cyclic voltammograms recorded at 400 ºC and under different gas compositions: 11.2 % CO_2, 4.7 % O_2 and 109 ppm SO_2 in N_2 (black), 11.2 % CO_2 and 4.7 % O_2 in N_2 (red). Inset: Potassium surface coverage for the cathodic and anodic scans under different gas compositions.

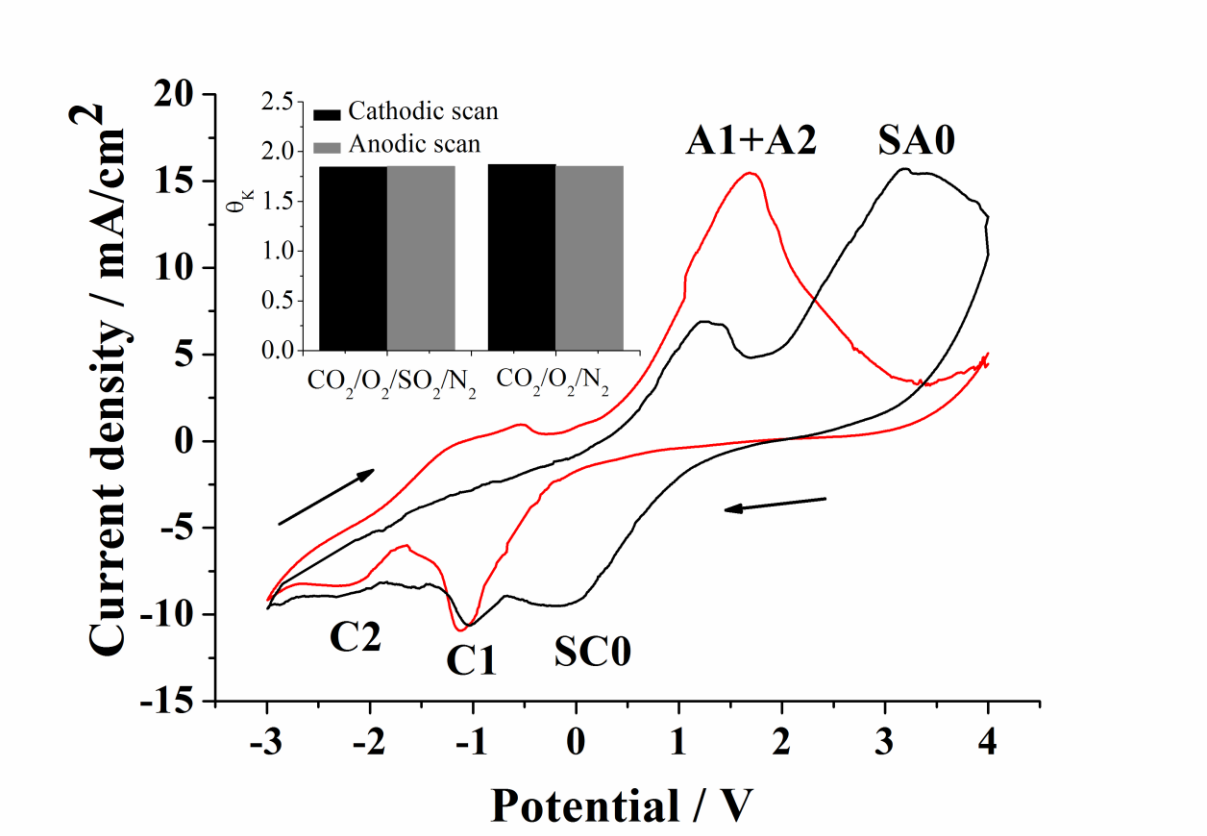

Fig. 8. Cyclic voltammograms recorded over Pt/K-βAl_2O_3 in the presence of CO_2 (11.2 %), O_2 (4.7 %) and SO_2 (109 ppm) at 400 ° C: 1st cycle (black), 2nd cycle (red), 3rd cycle (blue). Inset: Potassium surface coverage corresponding to the cathodic C1 peak (carbonate formation) over cycles.

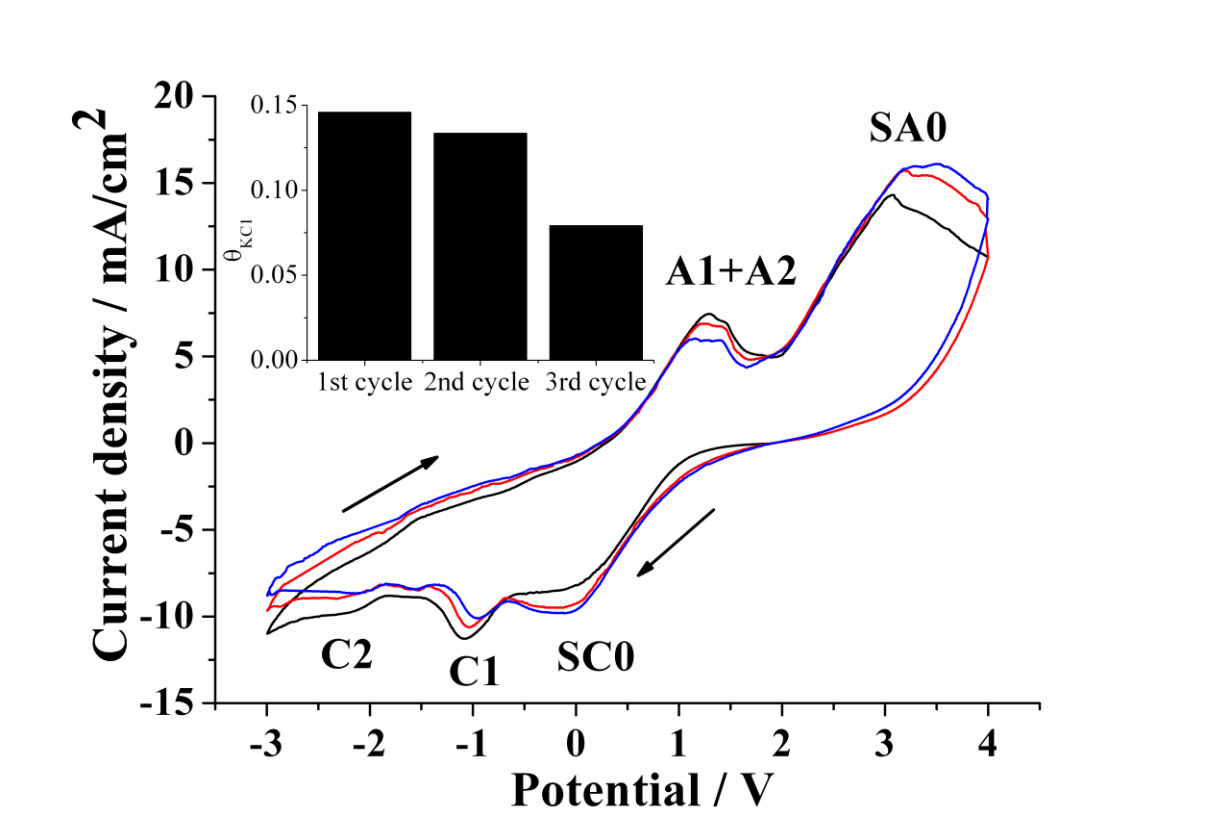

Fig. 9. Effect of NO on electropromoted CO_2 capture over Pt/K-βAl_2O_3. Cyclic voltammograms recorded at 400 ºC and under different gas compositions: 11.2 % CO_2, 4.7 % O_2 and 492 ppm NO in N_2 (black), 11.2 % CO_2 and 4.7 % O_2 in N_2 (red). Inset: Potassium surface coverage for the cathodic and anodic scans under different gas compositions.

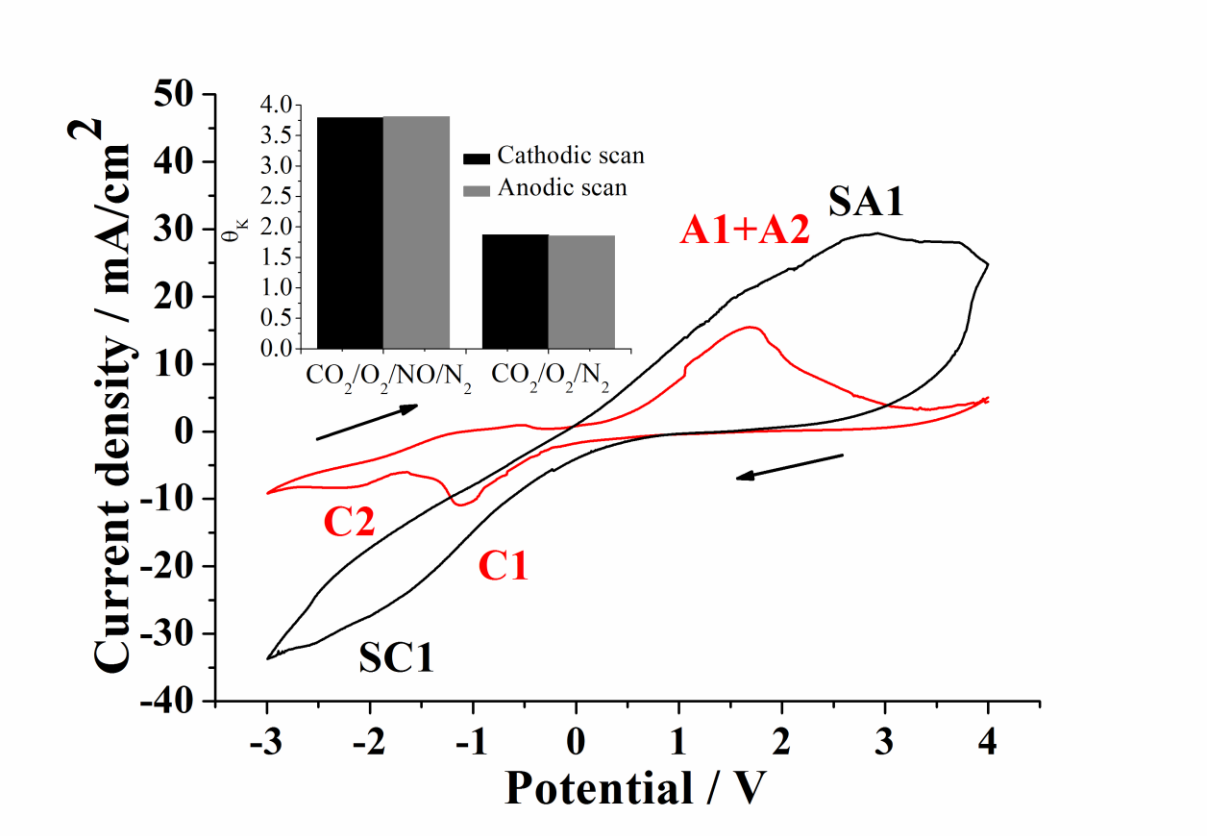

Fig. 10. Cyclic voltammograms recorded over Pt/K-βAl_2O_3 in the presence of CO_2 (11.2 %), O_2 (4.7 %) and NO (492 ppm) at 400 ^{o} C: 1st cycle (black), 2nd cycle (red), 3rd cycle (blue).

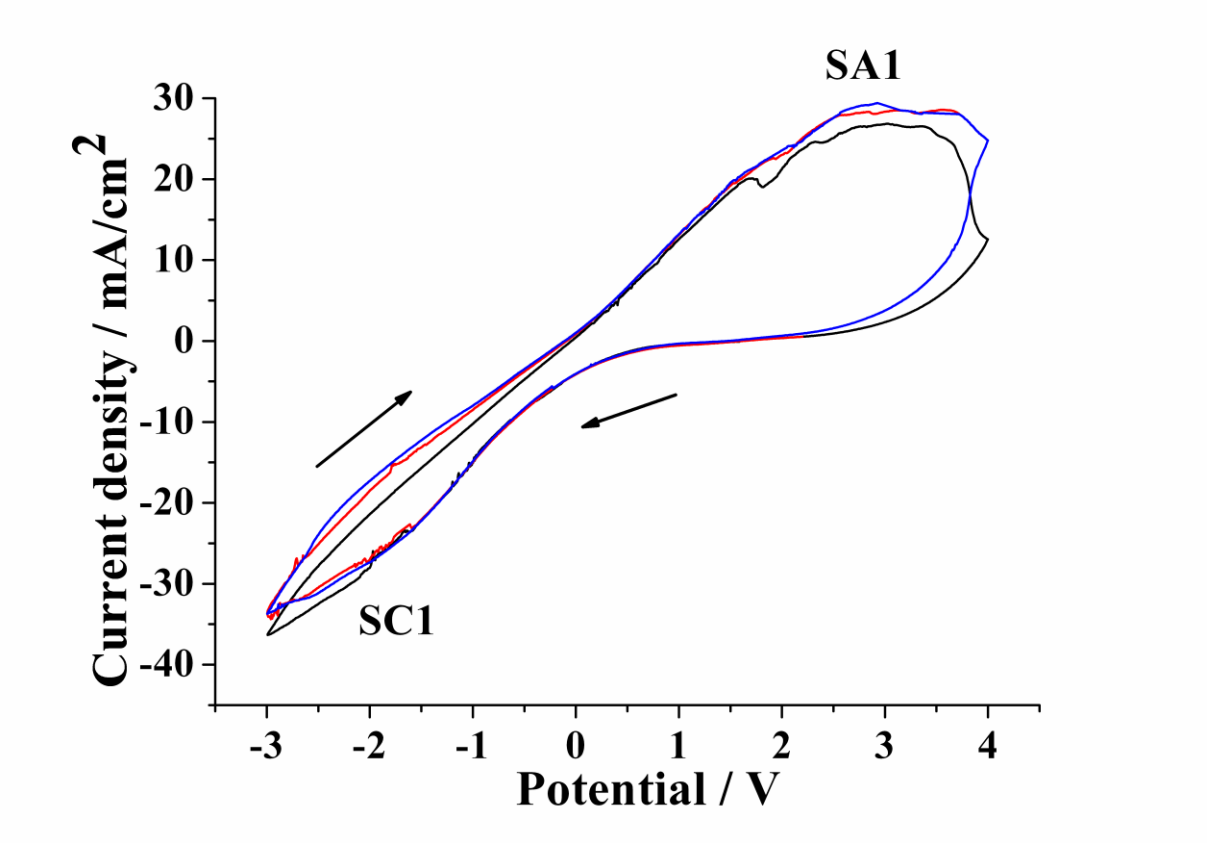

Fig. 11. Comparative XRD spectra of the Pt catalyst-working electrode film as prepared (black) and after reduction and testing (red).

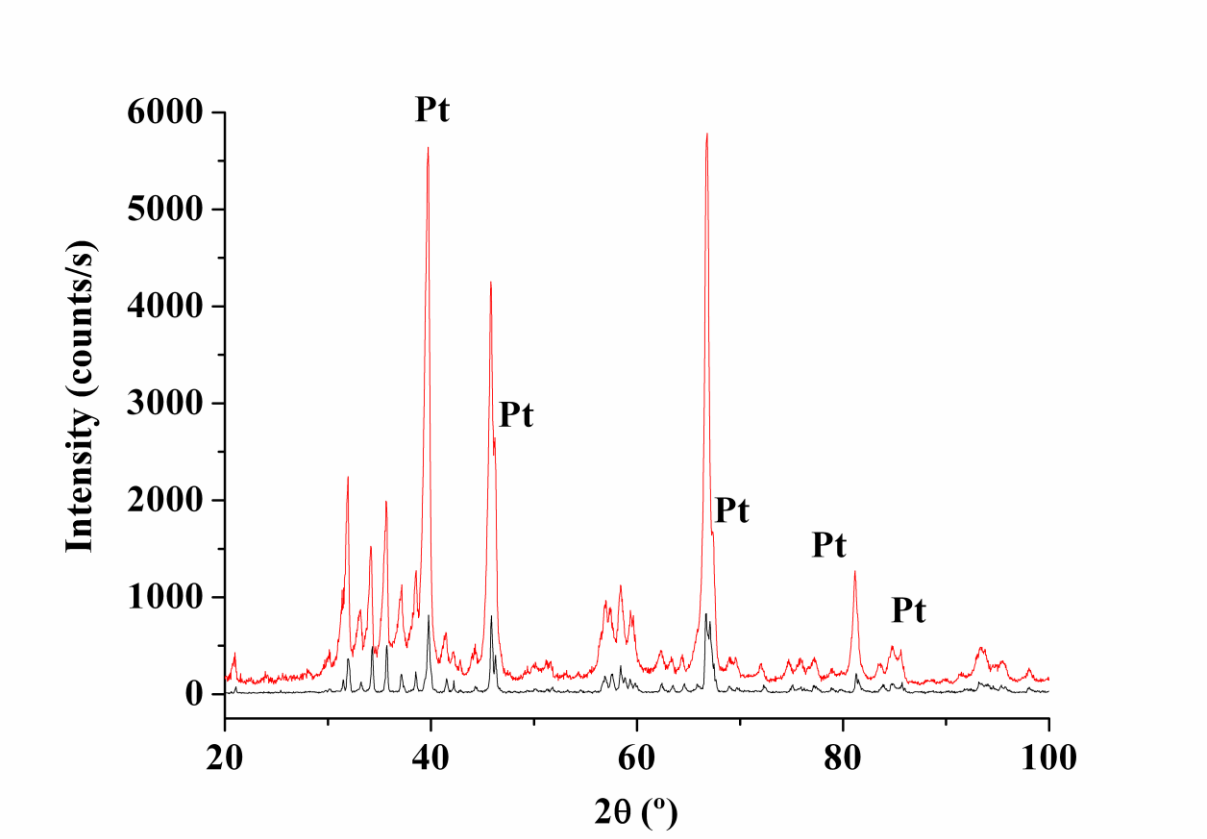

Tables

Table 1. Electropromoted adsorption-desorption tests. Feed gas compositions.

Gas composition (v/v)
11.2 % CO_2 in N_2
11.2 % CO_2 , 4.7 % O_2 in N_2
11.2 % CO_2 , 4.7 % O_2, 10 % H_2O in N_2
11.2 % CO_2 , 4.7 % O_2, 500 ppm N_2O in N_2
11.2 % CO_2 , 4.7 % O_2, 109 ppm SO_2 in N_2
11.2 % CO_2 , 4.7 % O_2, 492 ppm NO in N_2